NATIONAL ADVISORY COMMITTEE FOR AERONAUTICS

TECHNICAL NOTE 3321

ANALYTICAL DETERMINATION OF THE MECHANISM OF AN AIRPLANE SPIN RECOVERY WITH DIFFERENT APPLIED YAWING MOMENTS BY USE OF ROTARY-BALANCE DATA

By Sanger M. Burk, Jr.

Langley Aeronautical Laboratory
Langley Field, Va.

NACA

Washington

December 1954

NATIONAL ADVISORY COMMITTEE FOR AERONAUTICS

TECHNICAL NOTE 3321

ANALYTICAL DETERMINATION OF THE MECHANISM OF AN AIRPLANE SPIN RECOVERY WITH DIFFERENT APPLIED YAWING MOMENTS BY USE OF ROTARY-BALANCE DATA

By Sanger M. Burk, Jr.

SUMMARY

An analytical investigation has been undertaken in an attempt to learn more about the factors which make up a spin and the mechanism of recovery therefrom. Use is made of rotary-balance data and a step-by-step integration process of Euler's equations of motion allowing six degrees of freedom. The present study makes an analysis of an airplane recovery from a right spin where constant applied antispin yawing moments due to application of 800 and 1,600 pounds of force at the left wing tip are considered.

The results of the investigation indicate that the spin recoveries for both applied yawing moments were fairly rapid (1 turn or less), the larger applied yawing moment effecting a somewhat faster recovery than the smaller one. When the smaller yawing moment was applied, oscillations occurred in the angle of attack and sideslip during the recovery and gradually increased until recovery was effected. When the larger yawing moment was applied, the angle of attack went rapidly to an unstalled condition; however, the angle of sideslip oscillated somewhat during the recovery. The recovery motion of the airplane appeared to be affected primarily by the action of the moments rather than the forces.

INTRODUCTION

The spinning and spin recovery of airplanes have always been and still are subjects of concern to manufacturers and pilots. The action and effectiveness of various applied moments in upsetting spin equilibrium and in bringing about satisfactory recovery is not clearly understood. Generally, dynamic scale models of airplanes are tested in the Langley 20-foot free-spinning tunnel as an expeditious means of determining whether the spin-recovery characteristics of the airplane are satisfactory. In the past it has not been possible to determine from

these tests how the various spin parameters change as the model recovers in the tunnel, although a twin-camera technique is currently being given consideration for obtaining such data. A few full-scale spin tests have been performed in the past with the airplane instrumented to determine various spin parameters; however, these tests were expensive, time consuming, and in many cases the data were not reliable because of difficulties encountered in properly instrumenting the airplane. An analytical study of the mechanism of spin recovery therefore appears to be desirable; however, the lack of the necessary six components of aerodynamic forces and moments through a wide range of spin attitude angles and rates of rotation generally has prevented an analytical investigation of the spin recovery in the past. In one instance, an analytical investigation of the spin recovery (ref. 1) was made by use of step-by-step calculations to determine the relative effectiveness of the rudder, elevator, and ailerons of an airplane in producing recovery from a developed spin. This investigation, however, was limited to the study of the initial motions immediately following the application of the controls and not of the entire motion until recovery was effected. Furthermore, the study was hindered because complete aerodynamic data were not available and estimated constant derivatives were used.

The present investigation is an analytical determination of the mechanism of airplane spin recoveries where different antispin yawing moments (such as might be produced by rockets) are applied to effect a spin recovery. This investigation utilizes aerodynamic forces and moments obtained in the Langley 20-foot free-spinning tunnel from a six-component rotary strain-gage balance over a wide range of spin attitudes. The data available were for a 1/10-scale model of an unswept-wing fighter airplane; also, results of tests of a 1/20-scale dynamic model of the same design were available. These aerodynamic data were used previously in an analytical investigation of a spin recovery by rudder reversal, the results of which have been published in reference 2.

Because of certain discrepancies in the rotary-balance data similar to those discussed in reference 3, some modifications were made to the aerodynamic data used in calculating the results in reference 2 and also the results in this paper; these discrepancies and modifications are discussed in detail herein. The discrepancies in the rotary-balance data are believed to be due to difficulties involved in setting the attitude of the model in order to obtain correctly the aerodynamic data for simulation of a steady spin.

SYMBOLS

The spin-recovery motions were calculated with respect to the body system of axes (fig. 1) and the forces and moments also were measured with respect to these axes. In addition, the calculated motions are

presented in terms of Euler's angles (fig. 2). In general, the positive directions of the forces, moments, velocities, and angles are shown in figures 1 and 2. For convenience, the wing span b was used to nondimensionalize all moment coefficients.

C_X longitudinal-force coefficient, $\frac{X}{\frac{1}{2}\rho V_R^2 S}$

C_Y lateral-force coefficient, $\frac{Y}{\frac{1}{2}\rho V_R^2 S}$

C_Z normal-force coefficient, $\frac{Z}{\frac{1}{2}\rho V_R^2 S}$

C_l rolling-moment coefficient, $\frac{L}{\frac{1}{2}\rho V_R^2 Sb}$

C_{m_b} pitching-moment coefficient (subscript denotes that the pitching moment was nondimensionalized by b rather than $\bar{c}$), $\frac{M}{\frac{1}{2}\rho V_R^2 Sb}$

C_n yawing-moment coefficient, $\frac{N}{\frac{1}{2}\rho V_R^2 Sb}$

X longitudinal force acting along X body axis, lb

Y lateral force acting along Y body axis, lb

Z normal force acting along Z body axis, lb

L rolling moment acting about X body axis, ft-lb

M pitching moment acting about Y body axis, ft-lb

N yawing moment acting about Z body axis, ft-lb

S wing area, sq ft

b wing span, ft

ρ air density, slugs/cu ft

R	spin radius in developed spin, distance from spin axis to center of gravity, ft
V_V	vertical component of velocity of airplane center of gravity (rate of descent), ft/sec
V_R	resultant linear velocity, ft/sec
u,v,w	components of velocity V_R along the X, Y, and Z body axes, respectively, ft/sec
Ω	resultant angular velocity (if axis of resultant rotation is vertical, $\Omega = \dot{\psi}_e$), radians/sec
p,q,r	components of angular velocity Ω about the X, Y, and Z body axes, respectively, radians/sec
μ	airplane relative-density coefficient, $\frac{m}{\rho S b}$
m	mass of airplane, $\frac{\text{weight}}{g}$, slugs
c	local chord, ft
$\bar{c}$	mean aerodynamic chord, ft
$x/\bar{c}$	ratio of distance of center of gravity rearward of leading edge of mean aerodynamic chord to mean aerodynamic chord
$z/\bar{c}$	ratio of distance between center of gravity and X body axis to mean aerodynamic chord (positive when center of gravity is below X body axis)
k_X,k_Y,k_Z	radii of gyration about X, Y, and Z body axes, respectively, ft
I_X,I_Y,I_Z	moments of inertia about X, Y, and Z body axes, respectively, slug-ft^2
$\frac{I_X - I_Y}{mb^2}$	inertia yawing-moment parameter
$\frac{I_Y - I_Z}{mb^2}$	inertia rolling-moment parameter

$\frac{I_Z - I_X}{mb^2}$ inertia pitching-moment parameter

$\left(\frac{I_X - I_Y}{I_Z}\right)pq$ gyrodynamic yawing term

$\left(\frac{I_Y - I_Z}{I_X}\right)qr$ gyrodynamic rolling term

$\left(\frac{I_Z - I_X}{I_Y}\right)pr$ gyrodynamic pitching term

g acceleration due to gravity, taken as 32.17 ft/sec^2

ψ_e total angular movement of X body axis from reference position measured in horizontal plane, positive when clockwise as viewed from above airplane, deg or radians as indicated

θ_e total angular movement of X body axis from horizontal plane measured in vertical plane, positive when airplane nose is above the horizontal plane, deg or radians as indicated

ϕ_e total angular movement of Y body axis from horizontal plane measured in the YZ body plane, positive when clockwise as viewed from rear of airplane (if X body axis is vertical, ϕ_e is measured from a reference position in the horizontal plane), deg or radians as indicated

(It should be noted that θ_e, ϕ_e, and ψ_e are Euler's space angles and can exceed 360°. The angle ψ_e is sometimes referred to herein as an azimuth angle.)

ϕ angle between Y body axis and horizontal measured in vertical plane, positive for erect spins when right wing downward and for inverted spins when left wing downward, deg

$\dot{\psi}_e$ resultant angular velocity about vertical axis, deg/sec or radians/sec as indicated

α angle of attack; angle between relative wind V_R projected into the XZ plane of symmetry and the X body axis, positive when relative wind comes from below XY body plane, deg

β	angle of sideslip; angle between relative wind V_R and plane of symmetry at center of gravity, positive when relative wind comes from right of plane of symmetry, deg
F	applied force, lb
t	time, sec

A dot over a symbol represents derivative with respect to time; for example, $\dot{u} = \frac{du}{dt}$.

GENERAL CONSIDERATIONS

A spin of an airplane is a motion wherein the airplane descends along a helical path with the mean angle of attack greater than the angle of attack at maximum lift. During the descent the spin may be steady or oscillatory (a condition where the airplane may either, in combination or individually, roll, yaw, and pitch) depending on both the aerodynamic and inertia characteristics of the airplane (ref. 4). In order to understand better the dynamics of the spin and spin recovery to be discussed in detail later, a more general examination of the motions and the forces and moments which cause them would appear to be desirable now. In a fully developed steady spin (i.e. no oscillations present) the aerodynamic forces and moments must be balanced by the inertia forces and moments produced by the rotating mass of the airplane in order to obtain a condition of dynamic equilibrium. Thus in a true steady spin all rates of change of velocities relative to the body axes are zero. All airplanes, however, apparently oscillate to some extent in the fully-developed spin and therefore accelerations relative to the body axes are always present.

An airplane is considered to have recovered from the spin when the angle of attack at the center of gravity of the airplane is below the stall. Recovery from a spin is generally attempted by movement of one or more of the airplane controls to upset the spinning equilibrium. Application of a yawing moment has been recognized in the past as an effective means of terminating spins, although recoveries of airplanes may be greatly affected by mass distribution to an extent that an applied pitching or rolling moment may be essential for recovery (ref. 5). In recovering from the spin the motion of the airplane may be quite varied. In some instances, the time rate of change of the azimuth angle $\dot{\psi}_e$ may decrease to zero and thus indicates that the rotation of the airplane has ceased. In other cases, the airplane may be turning or rolling, a condition where $\dot{\psi}_e$ would not be zero. These types of motion could be classified as a spiral or aileron roll, respectively. Also the airplane may

roll or pitch rapidly to an inverted attitude for which condition $\dot{\psi}_e$ is not zero.

The time for recovery of the airplane is measured from the time at which the moment is applied until the spin is terminated. The number of turns for recovery which is normally used in the evaluation of spin recoveries in the Langley free-spinning tunnel investigations can be obtained from the maximum azimuth angle ψ_e attained during recovery. If the airplane recovers from the spin in $2\frac{1}{4}$ turns or less after the moment is applied, the recovery is considered to be satisfactory.

PROCEDURE

Method of Analysis

In order to evaluate the various factors which influence the spin-recovery motion, calculations were made by using the six equations of motion. A step-by-step rather than an analytic solution of these equations of motion was made because the gyrodynamic terms are nonlinear in these equations since these terms are the product of two velocities, and in addition the aerodynamic terms are nonlinear because of the large angles involved in the spin recovery. Euler's step-by-step method was used as presented in reference 6. Euler's equations of motion for six degrees of freedom (ref. 7) are so arranged that the terms on the left side of the equations are the aerodynamic and gravity component terms and those on the right side are the inertia terms, including centrifugal and gyrodynamic terms. These equations are:

$$\left.\begin{aligned} X - m(g \sin \theta_e) &= m(\dot{u} - rv + qw) \\ Y + m(g \cos \theta_e \sin \phi_e) &= m(\dot{v} - pw + ru) \\ Z + m(g \cos \theta_e \cos \phi_e) &= m(\dot{w} - qu + pv) \\ L &= \dot{p}I_X - (I_Y - I_Z)qr \\ M &= \dot{q}I_Y - (I_Z - I_X)pr \\ N &= \dot{r}I_Z - (I_X - I_Y)pq \end{aligned}\right\} \quad (1)$$

For this investigation the body axes are assumed to be the principal axes and, consequently, the product-of-inertia terms are zero.

The components of the weight along the body axes are defined by the use of Euler's angles. (See fig. 2.) By using these particular angles, a body can be positioned in space in the same attitude regardless of the sequence of angular movement.

For the calculations in this paper, a yawing moment is applied to the airplane to effect a spin recovery. This yawing moment is obtained by applying a force at the left wing tip of the airplane, which is spinning to the right. Since a force is applied at the wing tip, a term must be added to the longitudinal-force equation, inasmuch as the force acts parallel to the X body axis, and a term must be added to the yawing-moment equation because the force produces a yawing moment about the Z body axis. If these two additional terms are included and the forces and moments are expressed in nondimensional form, equations (1) may be solved for the linear and angular accelerations to be used in the step-by-step calculations as follows:

$$\left.\begin{aligned}
\dot{u} &= \frac{V_R^2}{2\mu b} C_X - g \sin \theta_e + rv - qw + \frac{F}{m} \\
\dot{v} &= \frac{V_R^2}{2\mu b} C_Y + g \cos \theta_e \sin \phi_e + pw - ru \\
\dot{w} &= \frac{V_R^2}{2\mu b} C_Z + g \cos \theta_e \cos \phi_e + qu - pv \\
\dot{p} &= \left(\frac{V_R^2}{2\mu k_X^2}\right) C_l + \left(\frac{I_Y - I_Z}{I_X}\right) qr \\
\dot{q} &= \left(\frac{V_R^2}{2\mu k_Y^2}\right) C_{m_b} + \left(\frac{I_Z - I_X}{I_Y}\right) pr \\
\dot{r} &= \left(\frac{V_R^2}{2\mu k_Z^2}\right) C_n + \left(\frac{I_X - I_Y}{I_Z}\right) pq + \frac{F\frac{b}{2}}{I_Z}
\end{aligned}\right\} \qquad (2)$$

In order to determine Euler's angles θ_e and ϕ_e for each step in the calculations, the following equations from reference 2 are used:

$$\frac{d}{dt}(-\sin \theta_e) = r(\cos \theta_e \sin \phi_e) - q(\cos \theta_e \cos \phi_e) \qquad (3a)$$

$$\frac{d}{dt}(\cos \theta_e \sin \phi_e) = p(\cos \theta_e \cos \phi_e) - r(-\sin \theta_e) \qquad (3b)$$

$$\frac{d}{dt}(\cos \theta_e \cos \phi_e) = q(-\sin \theta_e) - p(\cos \theta_e \sin \phi_e) \qquad (3c)$$

The same method as used previously in reference 6 (Euler's method) is used to determine the values of these angles. The third Euler angle ψ_e is determined from the following equation given in reference 2 or 8:

$$\dot{\psi}_e = \frac{\dot{\phi}_e - p}{\sin \theta_e} \qquad (4)$$

By graphically integrating $\dot{\psi}_e$ over the time interval used, the change in ψ_e was obtained for that time period.

Consideration of Rotary-Balance Data

The aerodynamic data used for the step calculations were obtained on the rotary balance of the Langley 20-foot free-spinning tunnel. The dimensions of the model are shown in figure 3 and the corresponding full-scale dimensions are presented in table I. The corresponding full-scale mass parameters, control settings, and initial developed-spin characteristics of the model are shown in table II. These data include no effects of accelerations such as are accounted for by the so-called dot stability derivatives. The effect of the dot stability derivatives on the spin and spin recovery are not known, since accelerations due to oscillations cannot be simulated on the rotary balance. In order to avoid extensive balance tests in the present investigation and also because of limitations of the equipment, certain liberties were taken with the control and attitude settings of the model. Thus, a minimum number of control settings were tested on the rotary-balance model. For zero sideslip, the rudder was set with, neutral, and against the spin, and for angles of sideslip other than zero, the rudder was maintained at neutral. In order to provide a rudder-with or rudder-against spin condition for angles of sideslip other than zero, the increments of aerodynamic forces and moments due to rudder deflection at zero sideslip were added to the values of the aerodynamic forces and moments obtained at other values of sideslip. In addition, because extensive tests would have been required, the spin radius was assumed to be zero throughout the present investigation. Some previous unpublished data obtained in the Langley 20-foot free-spinning tunnel have indicated that, for apparent steady-spin conditions, the rotary-balance data were not appreciably different when a value other than zero was used for spin radius and when the spin radius was set at zero and α, β, and Ω were adjusted to have the values that they would have had if a spin radius other than zero had been used. It is possible, however, that if the radius of turn should become relatively large, the use of zero-spin-radius balance data in computing the spin recovery may have some effect on that part of the calculated motion.

Results of the investigation of reference 3, in which a model was mounted on the rotary balance at attitudes and control settings corresponding to those for apparently steady spin conditions obtained previously with a dynamic model, indicated that the aerodynamic data obtained were inconsistent with the assumption of a steady spin in that the aerodynamic forces and moments did not balance the inertia forces and moments. Because of this discrepancy, it would be necessary to modify either the aerodynamic data or the inertia characteristics of the airplane to simulate equilibrium in a steady spin. In the present investigation also, the aerodynamic and inertia forces and moments were not in balance for the initial steady spinning motion, and thus it was arbitrarily decided to modify the aerodynamic data by adding the required increment to each force and moment coefficient to indicate equilibrium in the steady spin. During the calculated spin-recovery motion, the aerodynamic data were modified by adding these same increments at each time interval. The use of these corrections does not mean that the balance gives erroneous readings; as previously mentioned, the inconsistencies are believed to be primarily due to difficulties involved in setting the attitude of the model in order to obtain correctly the aerodynamic data for simulation of a steady spin.

Some of the modifications or corrections to the aerodynamic data were rather large; however, the corrections made to the aerodynamic data did not change the slopes of curves plotted from the aerodynamic data with respect to the variables of the motion, and these corrections might therefore be considered to represent a change in the aerodynamic characteristics of the model in order to obtain equilibrium in a steady spin without changing the stability of the airplane in the spin. Thus, if the stability of the airplane in a spin determines the more important characteristics of the spin-recovery motion, the calculated recovery may represent fairly well that of the actual rotary-balance model tested.

CONDITIONS FOR CALCULATIONS

With the addition of the incremental corrections to the aerodynamic data, the airplane is considered to be in a condition of spinning equilibrium at zero time; the airplane also is considered to be spinning to the right at an altitude of 15,000 feet. For the particular spin considered in the calculations, the rudder was with the spin, the elevator up, and the ailerons against the spin. The initial developed spin characteristics of the airplane were obtained by taking the average values of the spin characteristics available from free-spinning test results of a 1/20-scale dynamic model of the unswept-wing fighter airplane and by assuming that these average values constitute a so-called steady spin. Since θ_e and ϕ_e are constant in a steady spin, $\dot{\theta}_e$ and $\dot{\phi}_e$ were zero.

For the purposes of comparison, recovery from the spin is attempted at zero time by applying 800 pounds of force at the wing tip for the first condition and 1,600 pounds of force for the second condition (equivalent to -20,000 and -40,000 foot-pounds of yawing moment, respectively). The force acts rearward on the left wing tip of the airplane so that an anti-spin yawing moment is applied about the Z body axis. The application of the force is parallel to the X body axis and acts continuously throughout the attempted spin recovery. Also, all controls are maintained in their original settings throughout the attempted spin recovery.

The time interval between steps in the simple Euler step-by-step procedure should be small enough to insure reasonably accurate results. Brief calculations were made with the time interval varied in order to arrive at a time interval that would give reasonably accurate results and yet would not unduly lengthen the calculations, which were performed by use of manually operated machines.

PRESENTATION OF RESULTS

The data are presented for the applied yawing moments and are in terms of the full-scale airplane motion. The results of the calculations are plotted in the figures as functions of time. The figures for the various variables are listed in the following table:

Variable	Figure
Linear accelerations, $\dot{u}$, $\dot{v}$, and $\dot{w}$	4
Angular accelerations, $\dot{p}$, $\dot{q}$, and $\dot{r}$	5
Angle of attack α and sideslip β	6
Euler space angles, θ_e and ϕ_e	7
Terms composing linear accelerations	8 and 9
Terms composing angular accelerations	10 and 11
Linear velocities, u, v, and w	12
Angular velocities, p, q, and r	13
Resultant and vertical velocity, V_R and V_V	14
Comparison of V_R and V_V	15
$\dot{\psi}_e$ and ψ_e	16

DISCUSSION

As previously mentioned, yawing moments of -20,000 and -40,000 foot-pounds were applied to the airplane to effect a recovery. Based on the resultant linear velocity in the steady-spin condition, these moments are equivalent to yawing-moment coefficients of -0.027 and -0.054, respectively, at the spin altitude.

Comparison of Varied Yawing Moments on Spin Recovery

The variation of the components of the linear and angular accelerations, or time rates of change of velocities, of the airplane (figs. 4 and 5) along and about the body axes which resulted from the application of -20,000 and -40,000 foot-pounds of yawing moment indicated that those produced by the -40,000 foot-pounds of yawing moment were larger throughout the entire spin recovery (t = 0 to 1.5 seconds) than those produced by the application of the -20,000 foot-pounds of yawing moment for the same period of time. However, the values at the end of the spin recovery (t = 3.45 seconds) for the condition for which -20,000 foot-pounds of yawing moment had been applied were considerably larger than those at the end of the spin recovery for the condition for which -40,000 foot-pounds of yawing moment had been applied.

With the application of the smaller antispin yawing moment, oscillations occurred in the angle of attack and sideslip (fig. 6) during the spin recovery which gradually increased until recovery was effected (α goes below stall angle). When the larger yawing moment was applied, the angle of attack went rapidly to an unstalled condition (fig. 6); however, the angle of sideslip oscillated somewhat during the recovery.

In order to ascertain how the attitude of the airplane was changing in space during the spin recovery, two of the Euler space angles (θ_e and ϕ_e) were plotted in figure 7 for both the -20,000 and -40,000 foot-pounds of applied yawing moment. In general, when the small antispin yawing moment was applied, the airplane rolled to the right 8° (t = 1.25 seconds) and then rolled to the left 40° (t = 2.35 seconds) as the airplane pitched down from a value of θ_e of -44° to -71°. At this point the airplane pitched up to -50° (t = 3.00 seconds) and then down to -77° where the calculations ended. In the meantime the airplane rolled very rapidly from the left to the right and continued to roll to the right until it rolled over inverted ($\phi_e > 90°$) at a time of 3.52 seconds.

When the large antispin yawing moment was applied, the airplane pitched down rapidly from -44° to -105° (t = 0 to 2.00 seconds) while rolling to the right 41°, even though the ailerons were against the spin. This behavior will be discussed in detail in a subsequent section. The fact that θ_e exceeded -90° indicated that the airplane had pitched over in an inverted position. Thus, one of the essential differences observed in the types of recoveries was that, with the application of the small antispin yawing moment, the airplane rolled over to an inverted position or low angle-of-attack attitude; whereas, with the application of large antispin yawing moment, the airplane pitched over to an inverted attitude.

It might be of interest to note that, when the small antispin yawing moment was applied, the resultant angular velocity Ω actually increased appreciably near the end of the spin recovery (fig. 13, t = 3.00 seconds)

and then decreased rapidly. This increase in Ω was the result of an increase in the rolling angular velocity p due to a rolling moment which was caused by negative sideslip previous to the increase in Ω. When the large antispin yawing moment was applied, Ω decreased continuously throughout the recovery (fig. 13).

Evaluation of Terms in Equations of Motion

The motion of an airplane in a spin recovery is very complex because many interrelated variables determine the motion, as indicated by Euler's equations of motion about and along the principal axes of the airplane. In order to understand the mechanism of recovery when different antispin yawing moments were applied, it appeared desirable to determine to what extent the different terms in Euler's dynamical equations affected the motion of the airplane in the present investigation.

Inasmuch as the attitudes in the spin and recovery are influenced by the linear and angular velocities, which in turn can be determined from the time rates of change of velocities, time histories of the terms that compose the linear accelerations along the X, Y, and Z body axes for both applied yawing moments were plotted in figures 8 and 9 and of the terms that compose the angular accelerations about the X, Y, and Z body axes were plotted in figures 10 and 11. The results in figures 8(a) and 9(a) indicated that the aerodynamic-longitudinal-force term $\frac{V_R^2}{2\mu b} C_X$ and the applied force term F/m were relatively small and therefore negligible in determining $\dot{u}$. Although the applied force was relatively small in this investigation, it may not always be insignificant. In figures 8(b) and 9(b), the results indicated that the gravity term $g \cos \theta_e \sin \phi_e$ and the aerodynamic lateral-force term $\frac{V_R^2}{2\mu b} C_Y$ were negligible in determining $\dot{v}$. All terms appeared to be important in determining $\dot{w}$. (See figs. 8(c) and 9(c).) The results presented in figures 10 and 11 indicated that all terms had approximately the same relative importance in determining the angular accelerations ($\dot{p}$, $\dot{q}$, and $\dot{r}$). For this investigation, it should be noted that, for a right erect spin and up to the time of recovery, u, w, p, and r were always positive (figs. 12 and 13).

Inasmuch as the aerodynamic longitudinal and lateral forces were negligible, the resultant aerodynamic force lay approximately along the Z body axis. Although the force of gravity did not affect the magnitude of $\dot{v}$ (eq. (2)) appreciably (because either ϕ_e was small or θ_e was large during the spin), the gravity terms were important in the equations for determining $\dot{u}$ and $\dot{w}$. Generally, the resultant aerodynamic force and the gravity force might affect the angles of attack and sideslip

through changes in the direction or magnitude of the resultant wind V_R (fig. 14). A comparison between the resultant and vertical linear velocities (V_R and V_V, respectively) in figure 15 showed no essential differences; thus the path of the airplane center of gravity, or the direction of the resultant wind, remained almost vertical in this investigation. The movement of the airplane center of gravity horizontally, therefore, was small. Also, because the path of the airplane center of gravity was essentially vertical in this investigation, the vertical component of the resultant aerodynamic force and the force of gravity appear to have no appreciable effect on the angles of attack and sideslip except through the influence of a change in dynamic pressure on the moments acting.

During most of the recovery the variation in the magnitude of the resultant linear velocity V_R (fig. 14) was small; therefore, the vertical component of the resultant force nearly balanced the force of gravity. Near the end of the recovery, especially for the condition where the -20,000 foot-pounds of yawing moment was applied, V_R increased appreciably as did V_V ($t = 3.0$ seconds); this increase indicated that the vertical component of the resultant aerodynamic force decreased.

The foregoing discussion indicates that, in this investigation, the forces were relatively unimportant in determining the spin-recovery motion and only the moments were probably significant.

Effect of the Application of -20,000 Foot-Pounds of Yawing Moment on the Mechanism of Spin Recovery

Application of -20,000 foot-pounds of yawing moment led to an immediate yawing angular deceleration (negative $\dot{r}$), which decreased the yawing angular velocity r (figs. 5 and 13, respectively). There was little immediate change in the rolling velocity p (fig. 13). Because of the decrease in r, the gyrodynamic pitching term $\left(\frac{I_Z - I_X}{I_Y}\right)pr$ in the equation for $\dot{q}$ was decreased immediately so that an unbalance between the gyrodynamic and aerodynamic pitching moments caused the airplane to pitch down immediately (negative q). (See figs. 10(b) and 13.) The sideslip, which had been slightly outward (negative) in the spin, immediately began to change until it became positive at a time of 0.80 second (fig. 6). This change in sideslip angle was primarily due to a reduction in the yawing velocity of the airplane associated with the applied yawing moment rather than due to an attitude change. A brief explanation of this relationship is as follows: The angle of sideslip for this phase of the motion (fig. 6, $t = 0$ to 0.80 second) is determined primarily by v since V_R is relatively constant $\left(\beta = \sin^{-1}\frac{v}{V_R}\right)$. Since v is determined by $\dot{v}$, β also is determined by $\dot{v}$. As previously mentioned, the important

terms in the equation for $\dot{v}$ (eq. (2)) are pw and ru. For this phase of the motion (t = 0 to 0.80 second), w and u (fig. 12) change only slightly and p is essentially constant (fig. 13); thus r, which varies appreciably (fig. 13), is the primary factor in determining the sideslip angle. Since r is determined by changes in $\dot{r}$, determination of the quantities that affect $\dot{r}$ is necessary. As indicated in equation (2), the yawing angular acceleration $\dot{r}$ can be affected by the constant applied yawing moment, the rolling and pitching velocities, and the aerodynamic yawing moment as influenced by attitude changes of the airplane. The results in figure 10(c), where the terms composing $\dot{r}$ are plotted, show that the applied yawing-moment term $\frac{F\frac{b}{2}}{I_Z}$ is considerably larger than the other terms for the time interval considered (t = 0 to 0.80 second). This result indicates that the applied yawing-moment term primarily determines the value of $\dot{r}$ and thus the sideslip angle.

As previously mentioned, p remained essentially constant for the time interval considered (fig. 13, t = 0 to 0.80 second) because $\dot{p}$ was almost zero (fig. 5). There was little rolling angular acceleration $\dot{p}$ because as the airplane pitched down (fig. 7) a positive increase in the gyrodynamic rolling moment resulted (fig. 10(a), t = 0.50 second). This increase, however, was quickly compensated for by a negative increase in the aerodynamic rolling moment (fig. 10(a), t = 0.50 second) apparently due to positive sideslip.

For this phase of the recovery (up to t = 0.80 second) although the gyrodynamic yawing term $\left(\frac{I_X - I_Y}{I_Z}\right)pq$ (fig. 10(c)) became positive (prospin) because of the combination of a negative pitching velocity and a negative loading $(I_X - I_Y)$, the yawing angular acceleration $\dot{r}$ (fig. 5) continued to remain negative; thus the yawing angular velocity r continued to be reduced (fig. 13). This reduction in r continued because the applied antispin yawing moment was considerably larger than the gyrodynamic yawing moment, and the aerodynamic yawing moment was very small for this phase of the recovery and therefore did not influence the motion to any appreciable extent. (See fig. 10(c).) It should be noted, however, that for a smaller applied yawing moment or a different loading the gyrodynamic and aerodynamic yawing moments may be much more significant.

As the angle of attack continued to decrease, the sideslip began to decrease positively (fig. 6, t = 1.20 seconds) and eventually became negative (fig. 6, t = 1.40 seconds). This decrease appears to occur primarily because the aerodynamic rolling moment due to dihedral effect eventually became slightly larger negatively than the gyrodynamic rolling moment (fig. 10(a), t = 0.80 second) and thus at some time previous to

the decrease in sideslip, the airplane began to roll slightly to the left about its X body axis. In addition, as the angle of attack decreased, the aerodynamic pitching term $\frac{V_R^2}{2\mu k_Y^2} C_{m_b}$ became smaller than the gyrodynamic pitching term $\left(\frac{I_Z - I_X}{I_Y}\right)pr$ (fig. 10(b), t = 1.50 seconds); eventually a nose-up pitching moment and a positive $\dot{q}$ resulted (fig. 5, t = 1.70 seconds). Therefore, the angle of attack eventually began to increase (fig. 6, t = 2.10 seconds). The failure of the gyrodynamic pitching moment to decrease as rapidly as the aerodynamic pitching moment apparently may be explained by the fact that, although there was a decrease in the yawing angular velocity r, there was also an appreciable increase in the rolling angular velocity p because of negative sideslip (dihedral effect). It should be noted that the angle of attack previously had been decreasing continuously from zero time until the end of 2.1 seconds. The angle of attack at this time was approximately 17.5°. The airplane was not considered to be out of the spin at this time, as it was still beyond the stalling angle of attack of the model from which the rotary balance data were obtained ($\alpha = 11°$); the azimuth angle ψ_e was still increasing (fig. 16).

As the angle of attack increased (fig. 6, t = 2.25 seconds), the negative sideslip continued to increase for a very short period and then began to decrease very rapidly (fig. 6, t = 2.50 seconds). This rapid decrease in the negative sideslip was due to changes both in the yawing motion and the attitude of the airplane and may be explained in the following manner. The use of a method of analysis similar to one employed previously in this report indicates that, from an examination of the equations for $\dot{v}$ and $\dot{r}$ and also figures 8, 10, 12, 13, and 14, the change in sideslip was due in part to the yawing motion resulting from the applied yawing moment and in part to the pitching up and rapid rolling to the right of the airplane about its X body axis because of a large positive aerodynamic rolling moment (fig. 10(a), t = 2.25 to 2.87 seconds). This large moment was primarily the result of a large dihedral effect and the fact that the resultant wind velocity V_R (fig. 14), which had not varied much up to this time, began to increase more rapidly throughout the rest of the recovery; thus the nagnitude of the aerodynamic moments was also increased. In addition, the antispin gyrodynamic rolling moment was very small (fig. 10(a), t = 2.25 to 3.00 seconds), almost insignificant, during this phase of the recovery as both q and r had small positive values (fig. 13). The pitching angular velocity q had a small positive value because of a large reduction in the aerodynamic nose-down pitching moment that occurred at t = 2.1 seconds (fig. 10(b)), where the angle of attack had reached a minimum (fig. 6). The yawing angular velocity r had a small positive value because of a large negative $\dot{r}$ (fig. 5) as a result of a combination of negative aerodynamic and gyrodynamic yawing moments and the applied negative yawing moment (fig. 10). The negative gyrodynamic

yawing moment resulted from a combination of a positive pitching velocity q (resulting from the airplane pitching up) and a negative mass loading $I_X - I_Y$ of the airplane. The aerodynamic yawing moment became negative primarily because of the yawing moment due to negative sideslip.

As the negative sideslip continued to decrease rapidly to zero, the rate of increase in the angle of attack began to decrease (fig. 6, $t = 2.75$ seconds) because the aerodynamic pitching moment was rapidly becoming larger negatively than the gyrodynamic pitching moment (fig. 10(b), $t = 2.50$ seconds). The increase in the aerodynamic pitching moment resulted from an increase in angle of attack and the increase in V_R, whereas the gyrodynamic pitching moment decreased positively because the product of the rolling and yawing angular velocities was decreasing (fig. 13).

The angle of attack eventually reached a peak at a time of 3.0 seconds (fig. 6) and then decreased very rapidly. The rapid decrease in angle of attack can be attributed to the relatively large negative aerodynamic pitching moment, which also peaked around 3.0 seconds (fig. 10(b)), and the fact that the gyrodynamic pitching moment decreased somewhat more rapidly than previously (fig. 10(b)). The rapid decrease of the gyrodynamic pitching moment occurred because the rolling angular velocity p was decreasing very rapidly (fig. 13, $t = 3.0$ seconds); thus the occurrence of a slight increase in the yawing angular velocity r was offset (fig. 13, $t = 3.25$ seconds). The rapid decrease in p may be attributed primarily to the large negative aerodynamic rolling moment due to dihedral effect and the fact that the ailerons, which were against the spin, became more effective at the very low angle of attack. The gyrodynamic rolling moment, which was positive (because q was negative), was nevertheless small compared to the large aerodynamic rolling moment, even though q and r both increased somewhat (fig. 13). This increase in r was the result of the aerodynamic yawing moment becoming positive primarily because of positive sideslip and the gyrodynamic yawing moment also becoming positive because, as previously mentioned, q was negative.

For the final phase of the recovery motion, the angle of attack decreased until it became negative at a time of approximately 3.55 seconds (fig. 6). The recovery of the airplane was considered to be completed at a time of 3.45 seconds where it became unstalled. The magnitude of the azimuth angle ψ_e (fig. 16) became a maximum at a time of 3.20 seconds; this indicates that the rotation of the airplane about a vertical axis had ceased. This result indicates that the airplane recovered in approximately one turn.

Effect of the Application of -40,000 Foot-Pounds of Yawing Moment on the Mechanism of Spin Recovery

When the large antispin yawing moment (-40,000 foot-pounds) was applied, like the smaller yawing moment, it immediately made the yawing angular acceleration $\dot{r}$ negative (fig. 5), which in turn reduced the yawing angular velocity r (fig. 13). The yawing angular velocity r decreased considerably faster for the larger applied antispin yawing moment than for the smaller one (fig. 13), even though the gyrodynamic and aerodynamic yawing moments generally were positive (pro-spin) for the entire spin recovery (fig. 11(c)). The rolling angular velocity p, in general, was affected in the same manner by the large applied antispin yawing moment as by the smaller one in that p did not vary appreciably during the first part of the recovery motion (fig. 13, up to $t = 0.85$ second). Inasmuch as r decreased rapidly, the gyrodynamic pitching term $\left(\frac{I_Z - I_X}{I_Y}\right)pr$ decreased rapidly (fig. 11(b)) and resulted in a large unbalance between the gyrodynamic and aerodynamic pitching moments. The airplane consequently began to pitch down rapidly. The sideslip, which was initially negative, changed rapidly until it became positive (fig. 6, $t = 0.50$ second). The change in sideslip was primarily due to a change in yawing velocity associated with the applied yawing moment (rather than due to an attitude change). This conclusion is obtained on the basis of the same method of analysis that was employed previously for the condition where the small yawing moment was applied.

The angle of attack was reduced continuously throughout the recovery from zero time (fig. 6). This differed from the motion which was produced when the small yawing moment was applied. Also, the resultant wind velocity V_R did not vary appreciably during the entire spin recovery (fig. 14) apparently because the recovery was so rapid that V_R did not have time to increase appreciably as it did when the small yawing moment was applied.

In the final phase of the recovery where the angle of attack was reduced until the airplane was below the stall, the rolling angular velocity p decreased very rapidly because of dihedral effect and because the ailerons which were set against the spin had become very effective at low angles of attack (fig. 13, $t = 1.5$ to 2.0 seconds). The airplane was considered to have recovered from the spin at a time of approximately 1.5 seconds when the airplane became unstalled even though the azimuth angle ψ_e continued to increase slightly throughout the recovery (fig. 16). This rotation to the right continued because in addition to the rudder being set so as to keep the airplane turning to the right the momentum of the airplane undoubtedly forced it to continue to rotate to the right for a short while. The airplane appeared to have recovered in approximately one-third of a turn (fig. 16).

Comparison Between Spin Recoveries Obtained by Applying a Constant Yawing Moment and by Rudder Reversal

A brief comparison has been made between a spin recovery calculated herein for a condition where -20,000 foot-pounds of constant yawing moment was applied and a recovery calculated in a previous investigation (ref. 2) wherein recovery was effected by rudder reversal from the same initial developed spinning condition as used in this paper. The yawing-moment coefficient due to rudder reversal was -0.0022 as compared to -0.027 for -20,000 foot-pounds of applied yawing moment.

In general, the variations of the time histories of the angle of attack and sideslip for the conditions where the yawing moment was applied and the rudder reversed were similar in that oscillations occurred in the angle of attack and sideslip which gradually increased until recovery was effected. The time for recovery when the rudder was reversed was approximately 5.7 seconds and the turns for recovery were 2; for the condition where -20,000 foot-pounds of yawing moment was applied the time for recovery was 3.55 seconds and the number of turns 1. The results obtained when the rudder was reversed also indicated that the airplane descended in an almost vertical path which was similar to the motion obtained when the -20,000 foot-pounds of yawing moment was applied.

CONCLUSIONS

An analytical investigation of the mechanism of airplane spin recovery with different applied antispin yawing moments indicates the following conclusions:

1. The recoveries were satisfactory for both applied yawing moments. Both recoveries were very rapid, the larger applied yawing moment effecting a somewhat faster recovery than the smaller one.

2. When the smaller yawing moment was applied, oscillations occurred in the angle of attack and sideslip during the recovery which gradually increased until recovery was effected. When the larger yawing moment was applied, the angle of attack went rapidly to an unstalled condition; however, the angle of sideslip oscillated somewhat during the recovery.

3. The recovery motion of the airplane appeared to be affected primarily by the action of the moments rather than the forces.

Langley Aeronautical Laboratory,
National Advisory Committee for Aeronautics,
Langley Field, Va., September 24, 1954.

REFERENCES

1. Bryant, L. W., and Jones, I. M. W.: Notes on Recovery From a Spin. R. & M. No. 1426, British A.R.C., 1932.

2. Scher, Stanley H.: An Analytical Investigation of Airplane Spin-Recovery Motion by Use of Rotary-Balance Aerodynamic Data. NACA TN 3188, 1954.

3. Stone, Ralph W., Jr., Burk, Sanger M., Jr., and Bihrle, William, Jr.: The Aerodynamic Forces and Moments on a 1/10-Scale Model of a Fighter Airplane in Spinning Attitudes As Measured on a Rotary Balance in the Langley 20-Foot Free-Spinning Tunnel. NACA TN 2181, 1950.

4. Stone, Ralph W., Jr., and Klinar, Walter J.: The Influence of Very Heavy Fuselage Mass Loadings and Long Nose Lengths Upon Oscillations in the Spin. NACA TN 1510, 1948.

5. Neihouse, A. I.: A Mass-Distribution Criterion for Predicting the Effect of Control Manipulation on the Recovery From a Spin. NACA WR L-168, 1942. (Formerly NACA ARR, Aug. 1942.)

6. Scarborough, James B.: Numerical Mathematical Analysis. Second ed., The Johns Hopkins Press (Baltimore), 1950, pp. 235-236.

7. Perkins, Courtland D., and Hage, Robert E.: Airplane Performance - Stability and Control. John Wiley & Sons, Inc., 1949, pp. 376-381.

8. MacMillan, William Duncan: Theoretical Mechanics. Dynamics of Rigid Bodies. First ed., McGraw-Hill Book Co., Inc., 1936, pp. 184-185.

TABLE I

DIMENSIONAL CHARACTERISTICS OF THE FULL-SCALE AIRPLANE

REPRESENTED BY THE 1/10-SCALE ROTARY-BALANCE MODEL

Wing span, ft	50.35
Overall length, ft	44.70
Wing:	
Area, sq ft	425.0
Airfoil section, root	NACA $65_{(112)}$-213
Airfoil section, tip	NACA $65_{(112)}$-213
Root-chord incidence, deg	2.5
Tip-chord incidence, deg	2.5
Aspect ratio	6.0
Sweepback of leading edge of wing, deg	0
Dihedral, leading-edge chord line, deg	6.0
Mean aerodynamic chord, $\bar{c}$, in.	115.00
Leading edge of mean aerodynamic chord rearward of leading edge of wing, in.	0
Flaps:	
Chord, percent of wing chord	18.75
Area (rearward of hinge line), percent of wing area	12.55
Span, percent of wing span	44.0
Ailerons:	
Chord, percent of wing chord	20.00
Area (rearward of hinge line), percent of wing area	5.90
Span, percent of wing span	44.8
Horizontal tail surfaces:	
Total area, sq ft	108.0
Span, ft	23.33
Elevator area (rearward of hinge line), sq ft	30.0
Distance from normal center of gravity to elevator hinge line, ft	24.20
Vertical tail surfaces:	
Total area, sq ft	36.0
Rudder area (rearward of hinge line), sq ft	13.2
Distance from normal center of gravity to top of rudder hinge line, ft	23.05

TABLE II

MASS PARAMETERS, CONTROL SETTINGS, AND DEVELOPED-SPIN CHARACTERISTICS FOR AIRPLANE CONFIGURATION

Mass parameters:	
Weight, lb	17,835
$x/\bar{c}$	0.212
$z/\bar{c}$	0.009
μ at 15,000 feet altitude	17.35
I_X, slug-ft^2	17,342
I_Y, slug-ft^2	37,920
I_Z, slug-ft^2	53,396
$\frac{I_X - I_Y}{mb^2}$	-147×10^{-4}
$\frac{I_Y - I_Z}{mb^2}$	-110×10^{-4}
$\frac{I_Z - I_X}{mb^2}$	257×10^{-4}
Control settings:	
Elevator, up (stick back), deg	20
Ailerons, against spin (stick left in spin to pilot's right), deg	± 14
Rudder with spin (right pedal forward in spin to pilot's right), deg	30
Developed spin characteristics:	
$\dot{\psi}_e$ or Ω, radians/sec	2.165
θ_e, radians/sec	0
ϕ_e, radians/sec	0
$-\theta_e$, deg	44
ϕ, deg	0.4
V_V, ft/sec	216
R, ft	6.62
α, deg	46
β, deg	-3.4

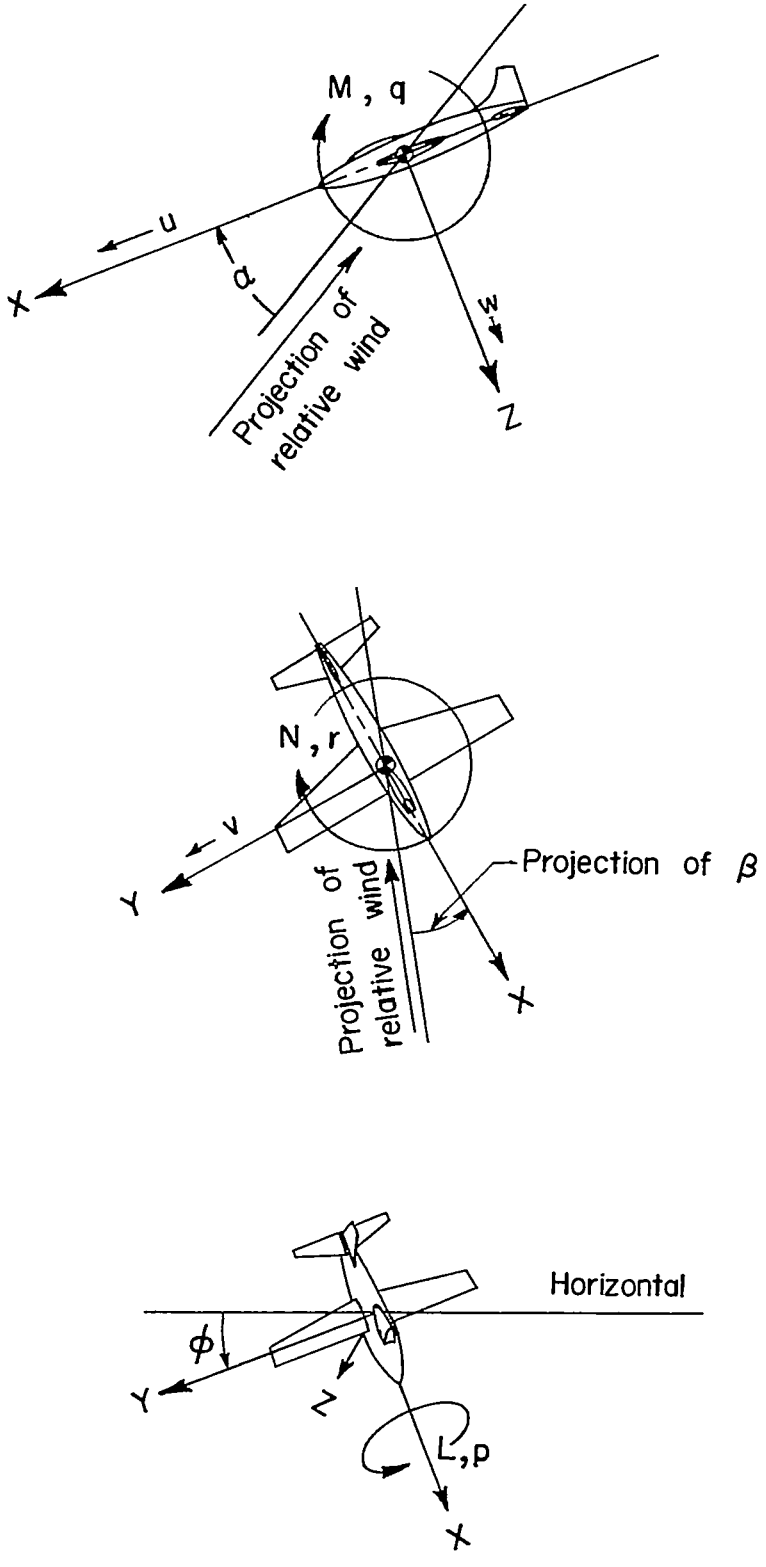

Figure 1.- Body system of axes. Arrows indicate positive directions of the forces, moments, velocities, and angles.

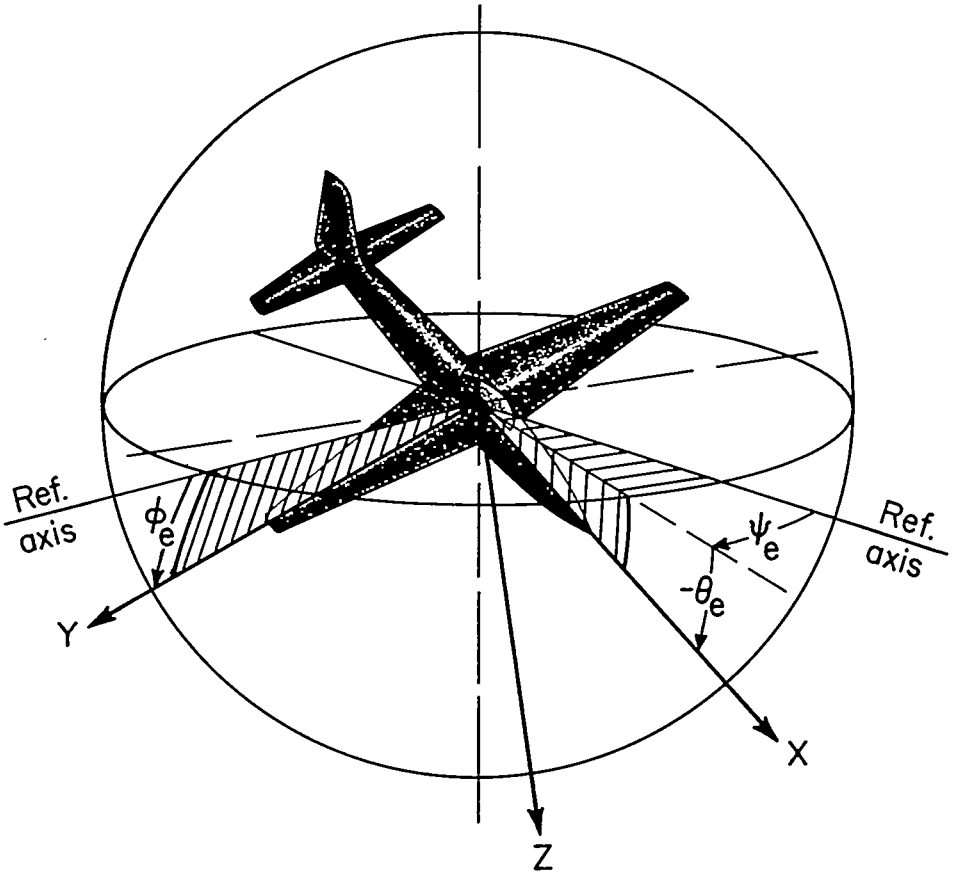

Figure 2.- Sketch illustrating Euler's space angles.

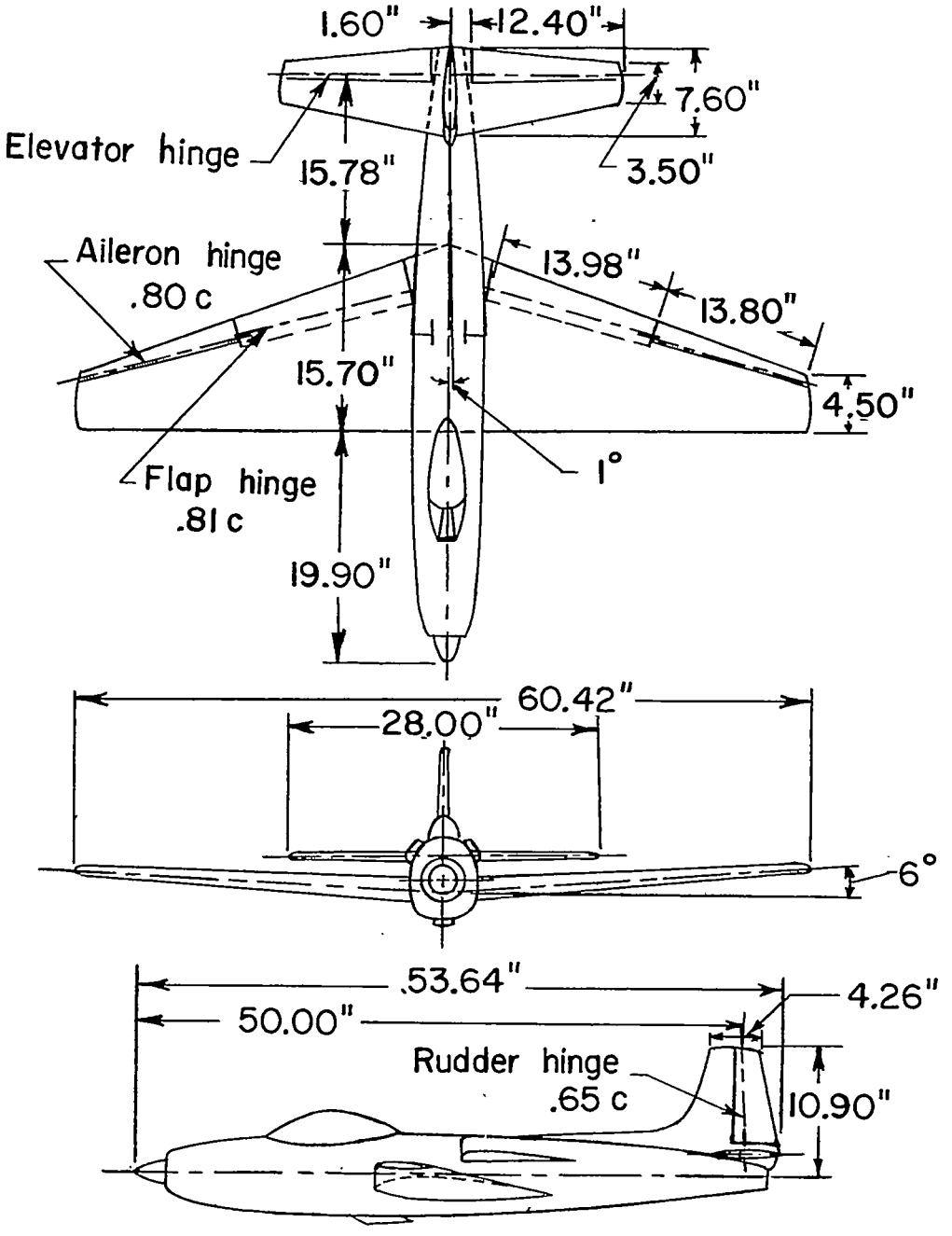

Figure 3.- Drawing of 1/10-scale rotary-balance model of fighter airplane.

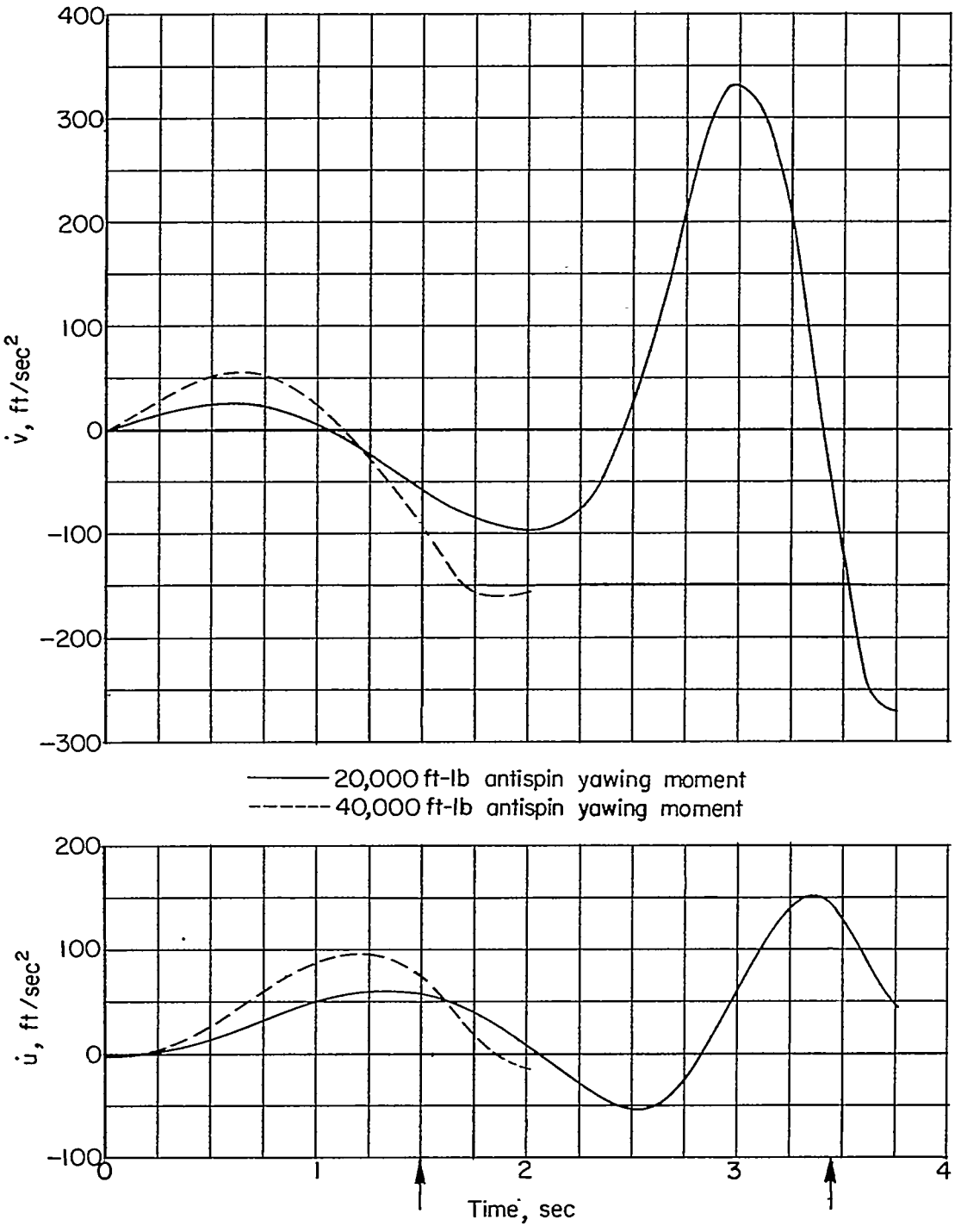

Figure 4.- Calculated time histories of the linear accelerations along the X, Y, and Z body axes for two applied antispin yawing moments. Time at which recovery is completed is indicated by vertical arrows in time scale.

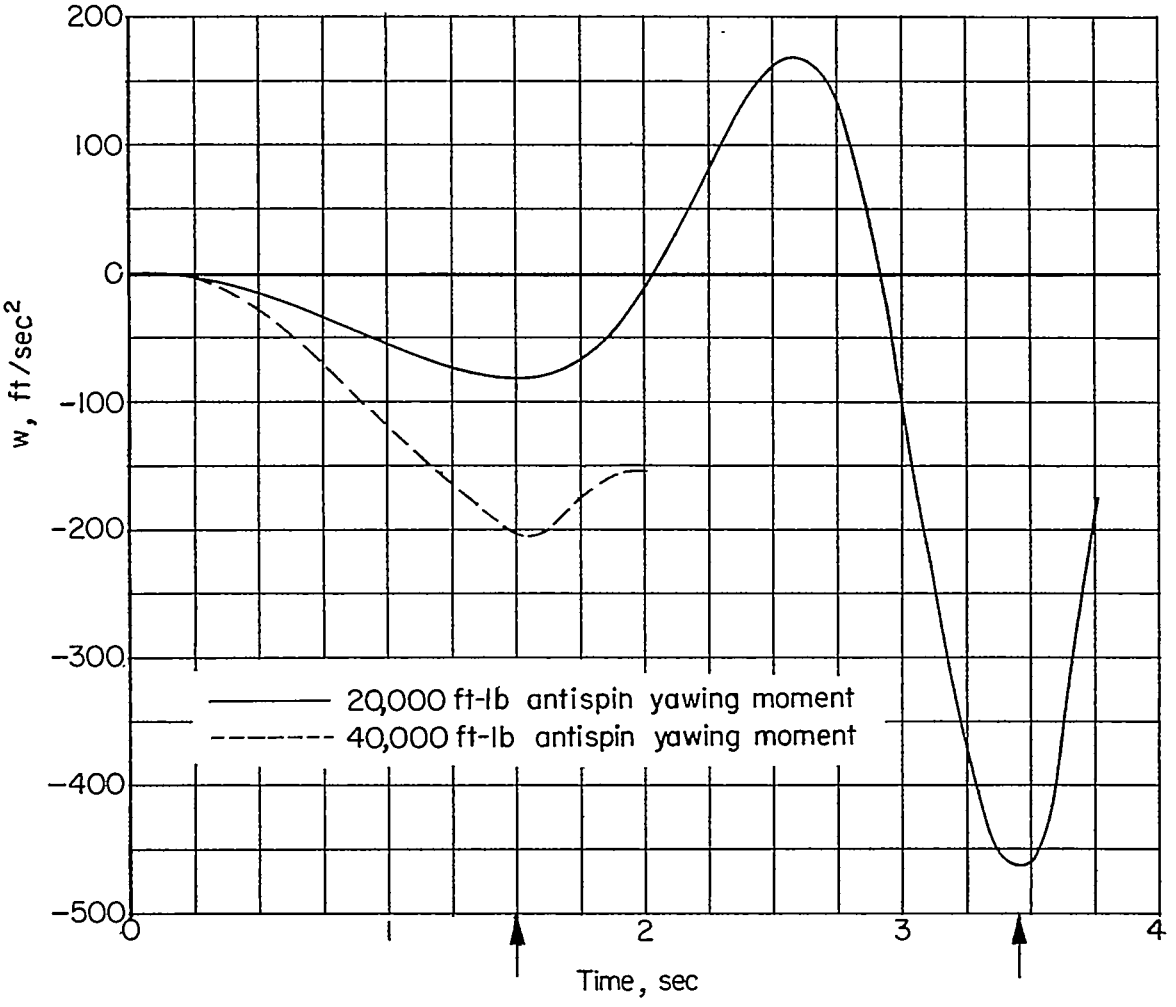

Figure 4.- Concluded.

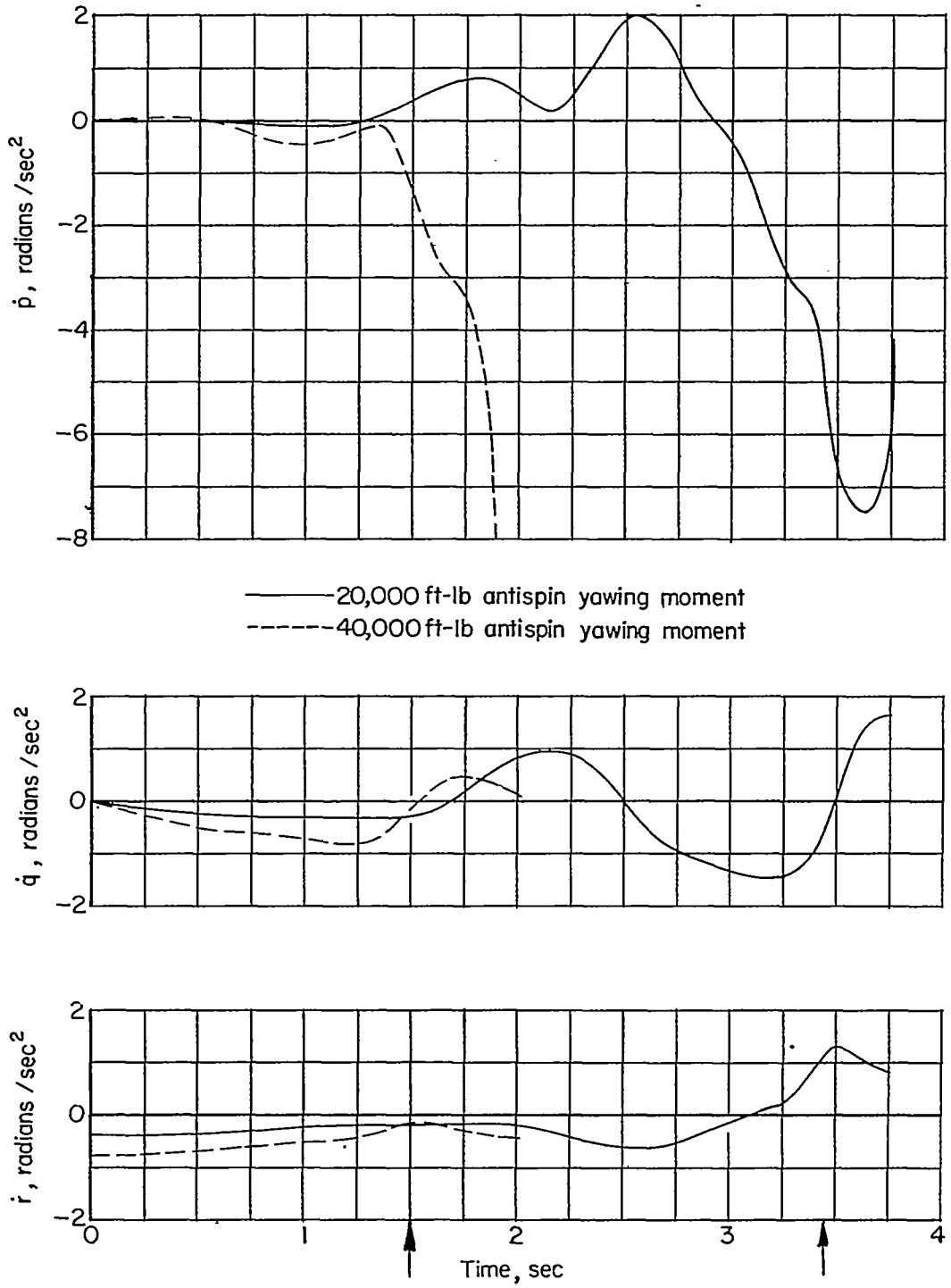

Figure 5.- Calculated time histories of the angular accelerations about the X, Y, and Z body axes for two applied antispin yawing moments. Time at which recovery is completed is indicated by vertical arrows in time scale.

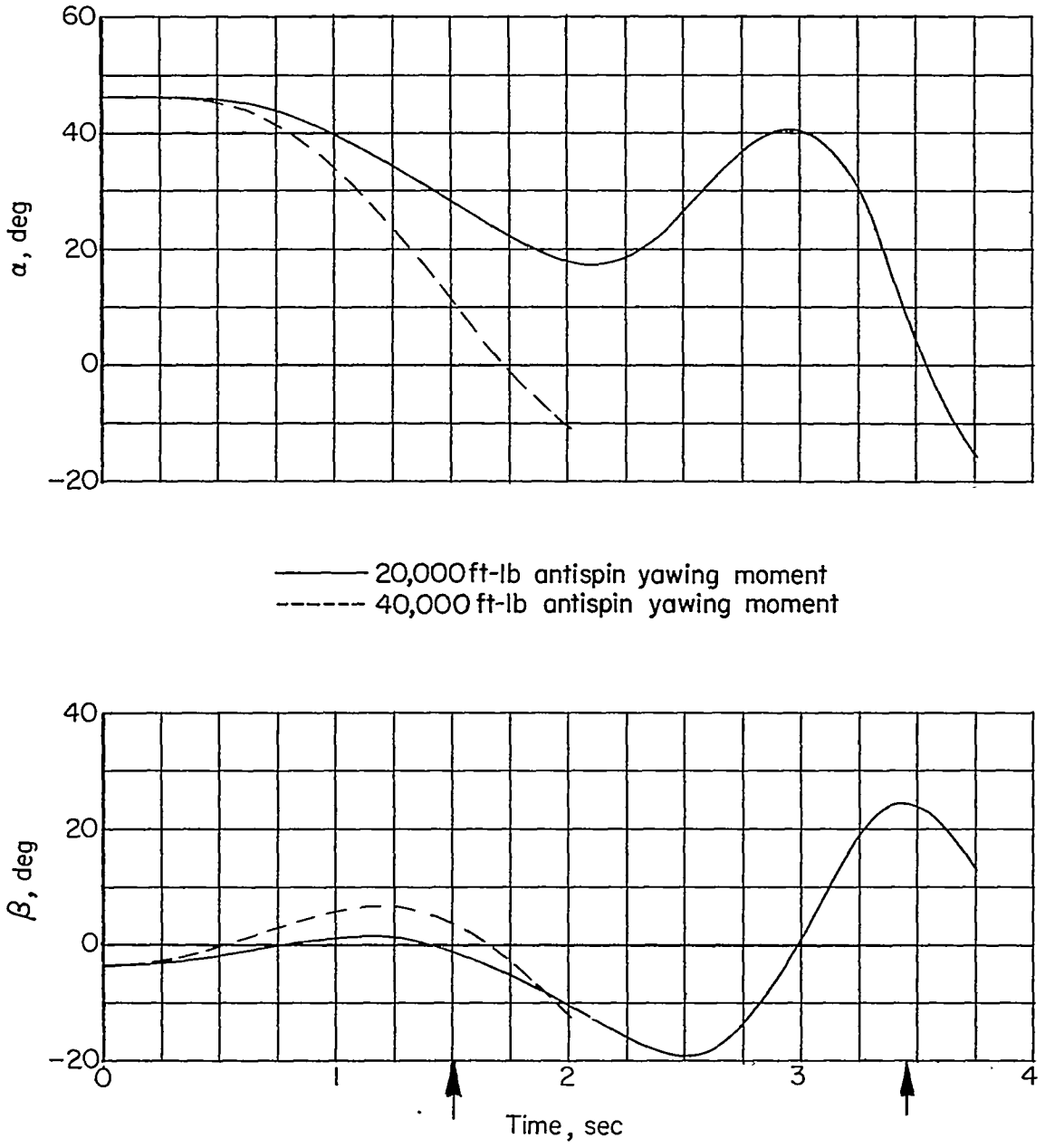

Figure 6.- Calculated time histories of the angle of attack and sideslip for two applied antispin yawing moments. Time at which recovery is completed is indicated by vertical arrows in time scale.

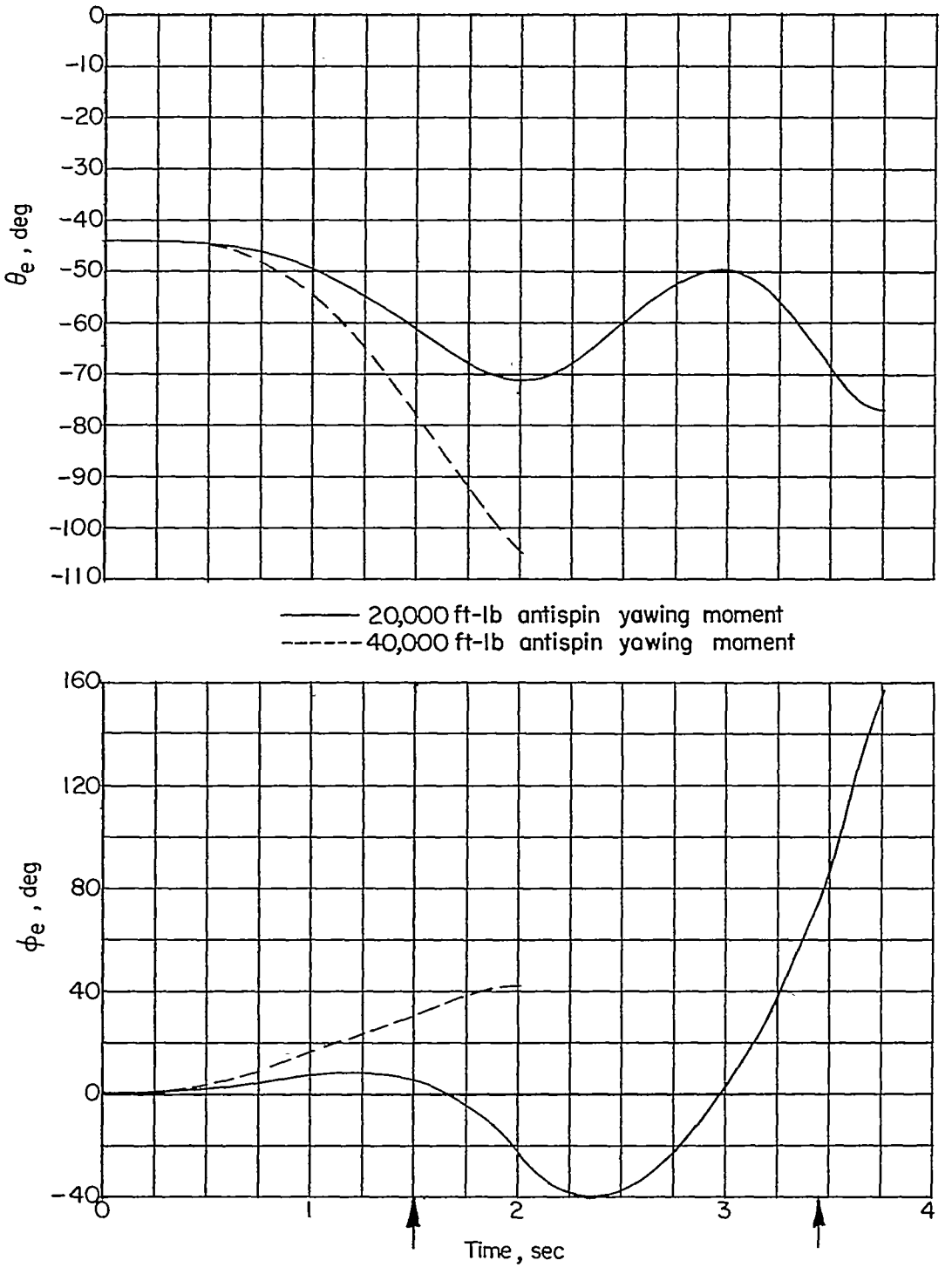

Figure 7.- Calculated time histories of θ_e and ϕ_e for two applied antispin yawing moments. Time at which recovery is completed is indicated by vertical arrows in time scale.

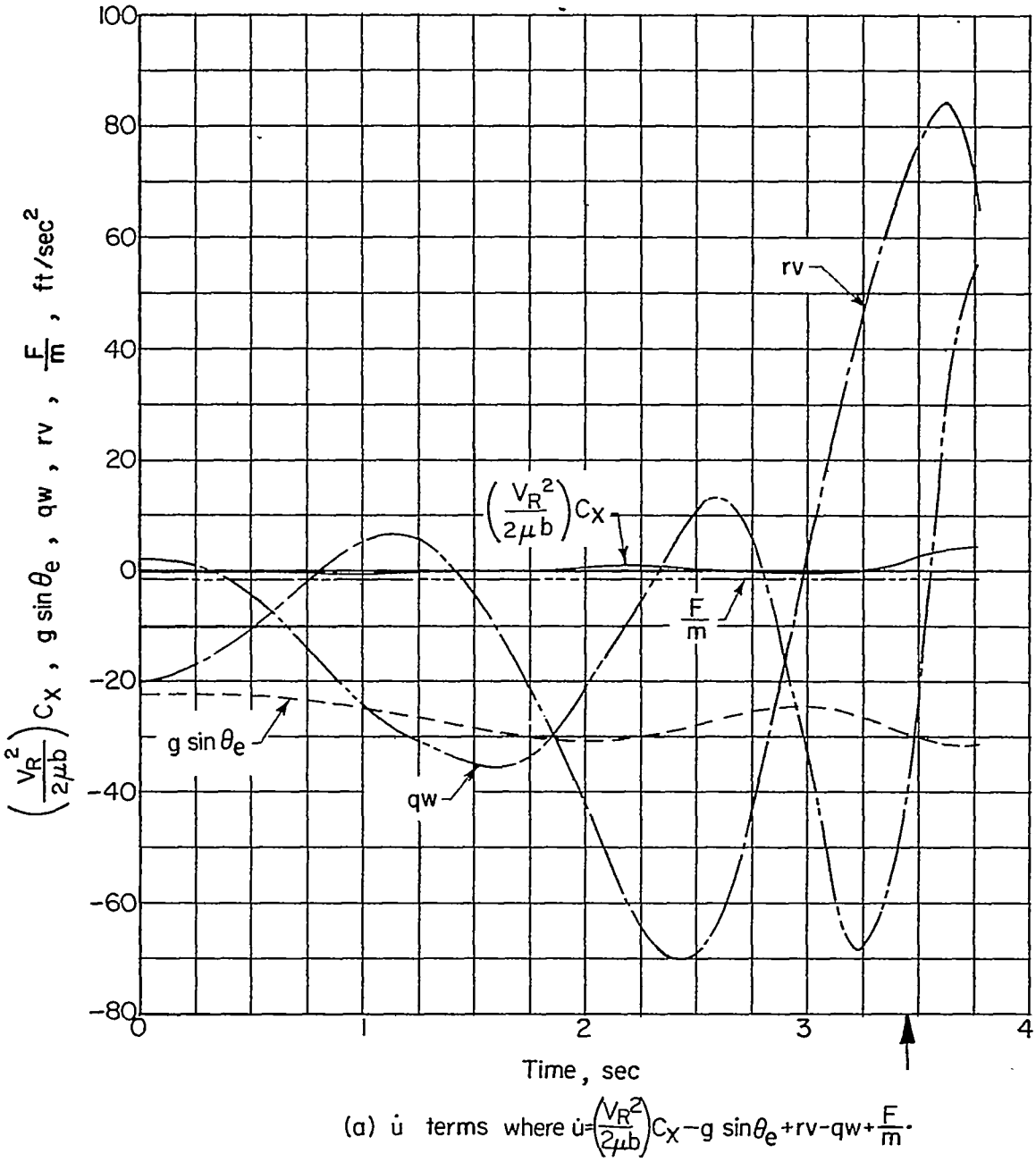

(a) $\dot{u}$ terms where $\dot{u}=\left(\frac{V_R^2}{2\mu b}\right)C_X - g \sin\theta_e + rv - qw + \frac{F}{m}$.

Figure 8.- Calculated time histories of the terms composing the linear accelerations along the X, Y, and Z body axes for the condition where 20,000 foot-pounds of antispin yawing moment was applied. Time at which recovery is completed is indicated by vertical arrow in time scale.

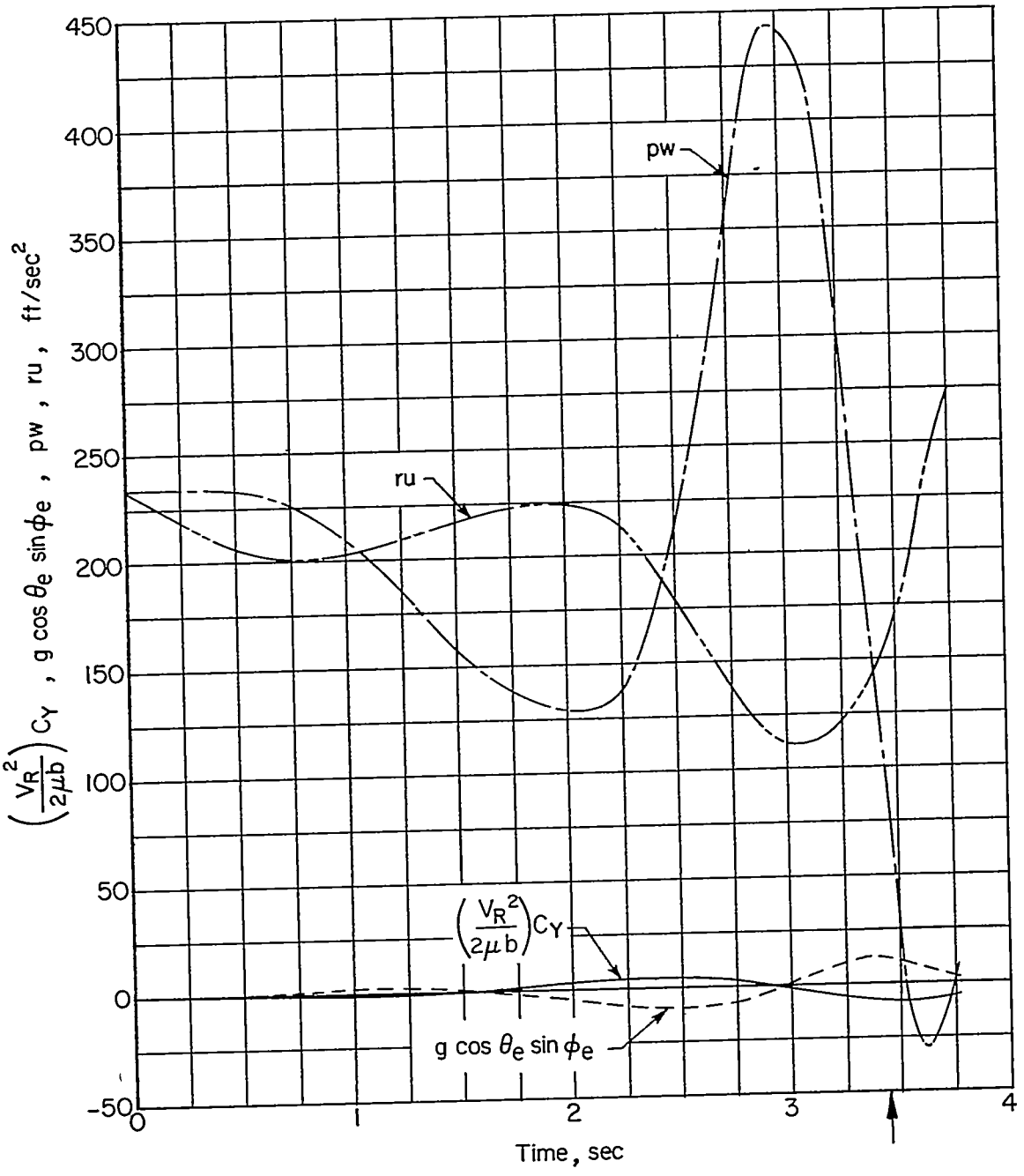

(b) $\dot{v}$ terms where $\dot{v}=\left(\frac{V_R^2}{2\mu b}\right)C_Y+g\cos\theta_e\sin\phi_e+pw-ru$.

Figure 8.- Continued.

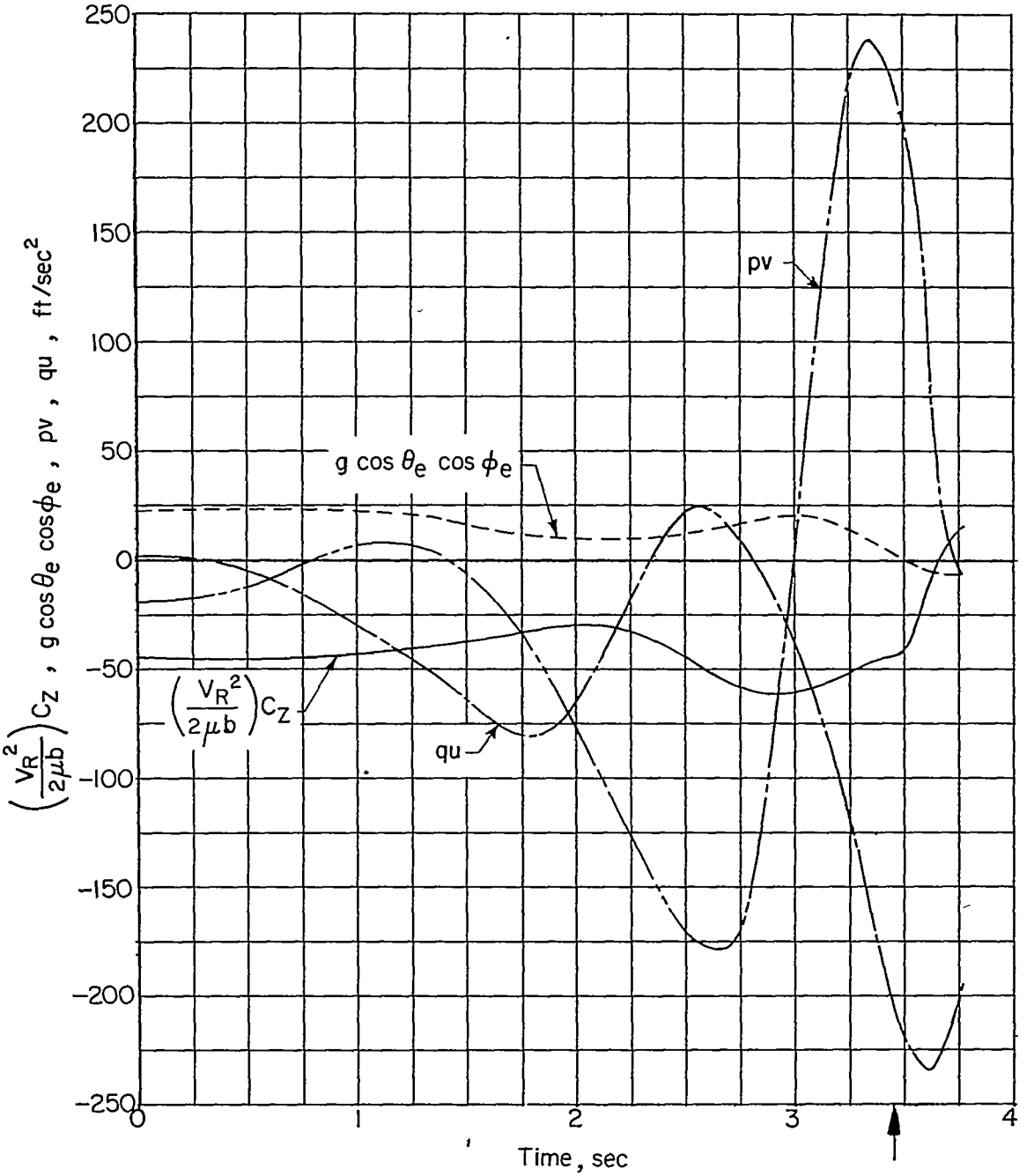

(c) $\dot{w}$ terms where $\dot{w}=\left(\frac{V_R^2}{2\mu b}\right)C_Z+g\cos\theta_e\cos\phi_e+qu-pv$.

Figure 8.- Concluded.

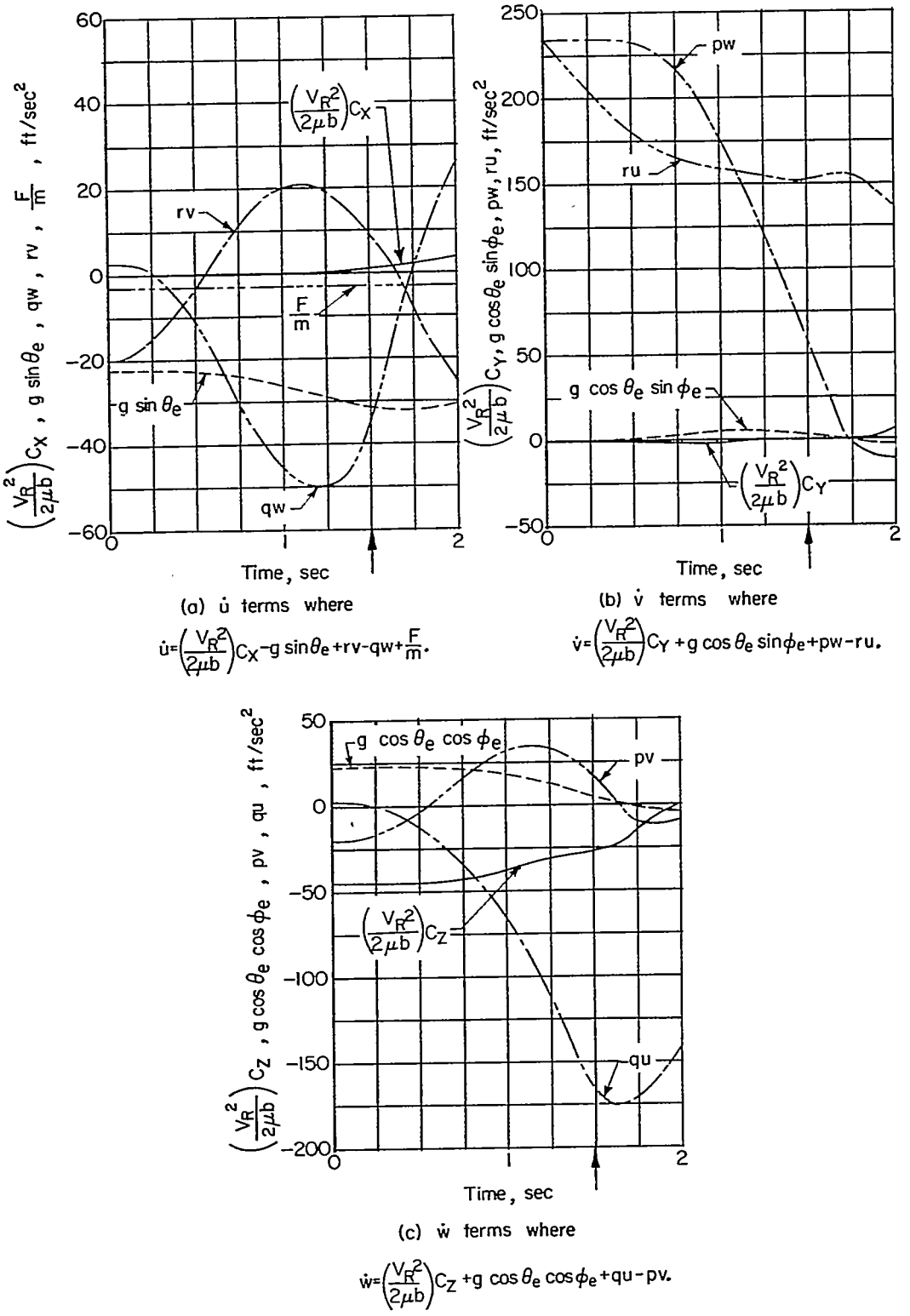

(a) $\dot{u}$ terms where

$$\dot{u}=\left(\frac{V_R^2}{2\mu b}\right)C_X-g\sin\theta_e+rv-qw+\frac{F}{m}.$$

(b) $\dot{v}$ terms where

$$\dot{v}=\left(\frac{V_R^2}{2\mu b}\right)C_Y+g\cos\theta_e\sin\phi_e+pw-ru.$$

(c) $\dot{w}$ terms where

$$\dot{w}=\left(\frac{V_R^2}{2\mu b}\right)C_Z+g\cos\theta_e\cos\phi_e+qu-pv.$$

Figure 9.- Calculated time histories of the terms composing the linear accelerations along the X, Y, and Z body axes for the condition where 40,000 foot-pounds of antispin yawing moment was applied. Time at which recovery is completed is indicated by vertical arrow in time scale.

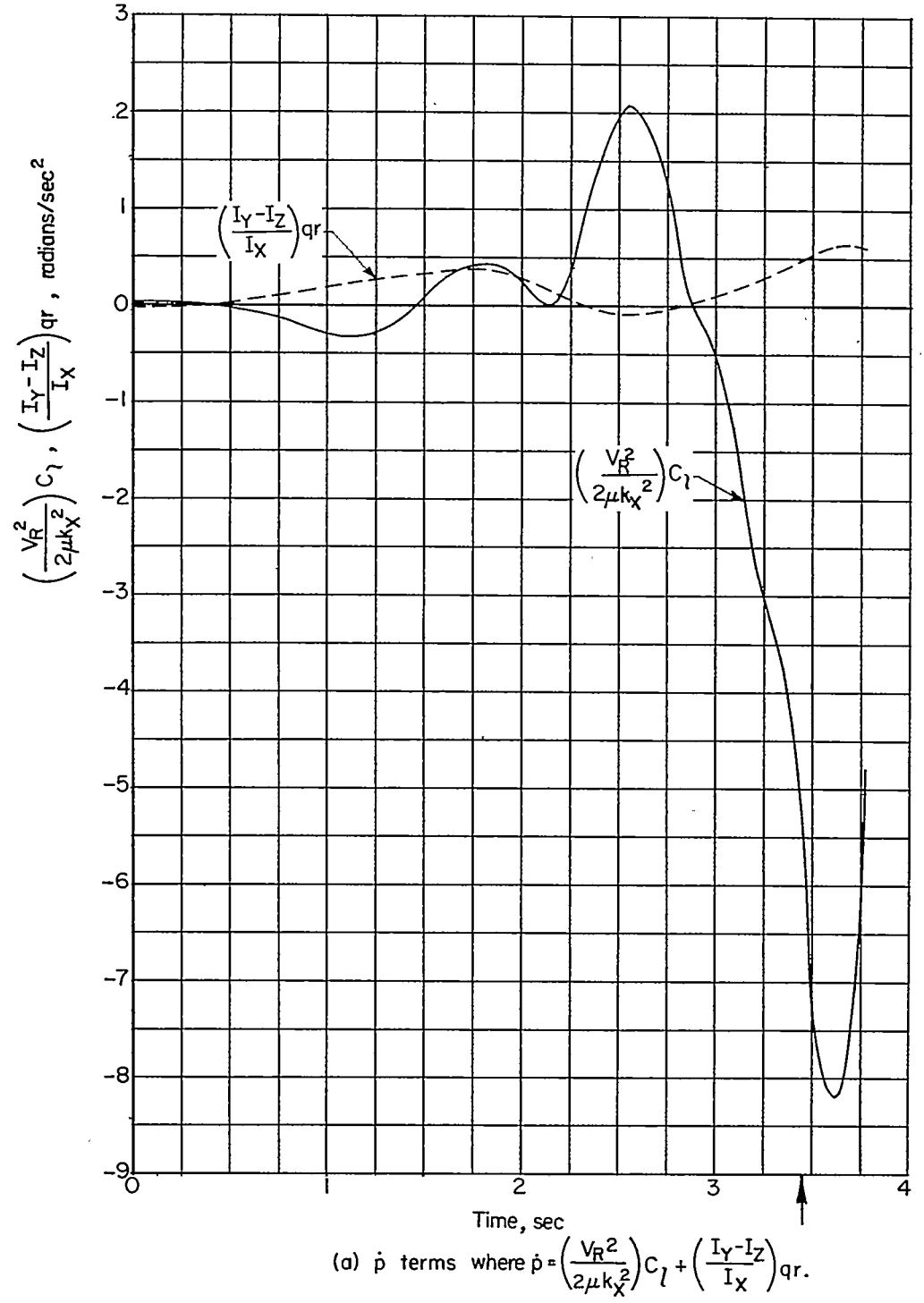

Figure 10.- Calculated time histories of the terms composing the angular accelerations about the X, Y, and Z body axes for the condition where 20,000 foot-pounds of antispin yawing moment was applied. Time at which recovery is completed is indicated by vertical arrow in time scale.

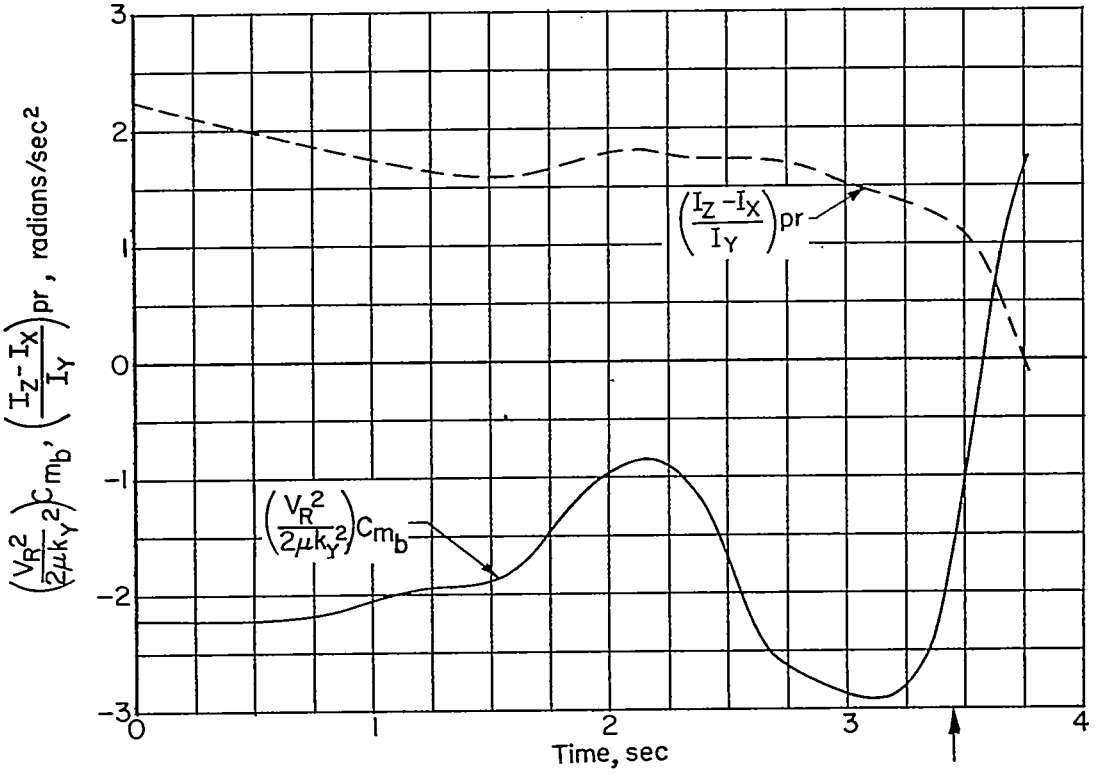

(b) $\dot{q}$ terms where $\dot{q} = \left(\frac{V_R^2}{2\mu k_Y^2}\right)C_{m_b} + \left(\frac{I_Z-I_X}{I_Y}\right)pr$.

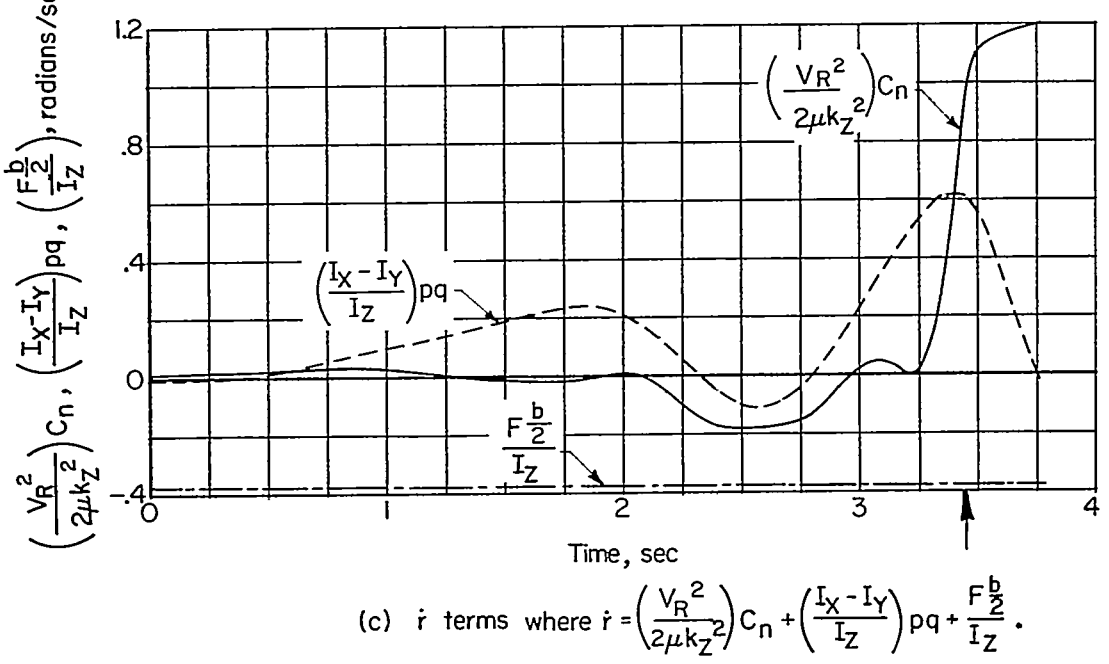

(c) $\dot{r}$ terms where $\dot{r} = \left(\frac{V_R^2}{2\mu k_Z^2}\right)C_n + \left(\frac{I_X-I_Y}{I_Z}\right)pq + \frac{F\frac{b}{2}}{I_Z}$.

Figure 10.- Concluded.

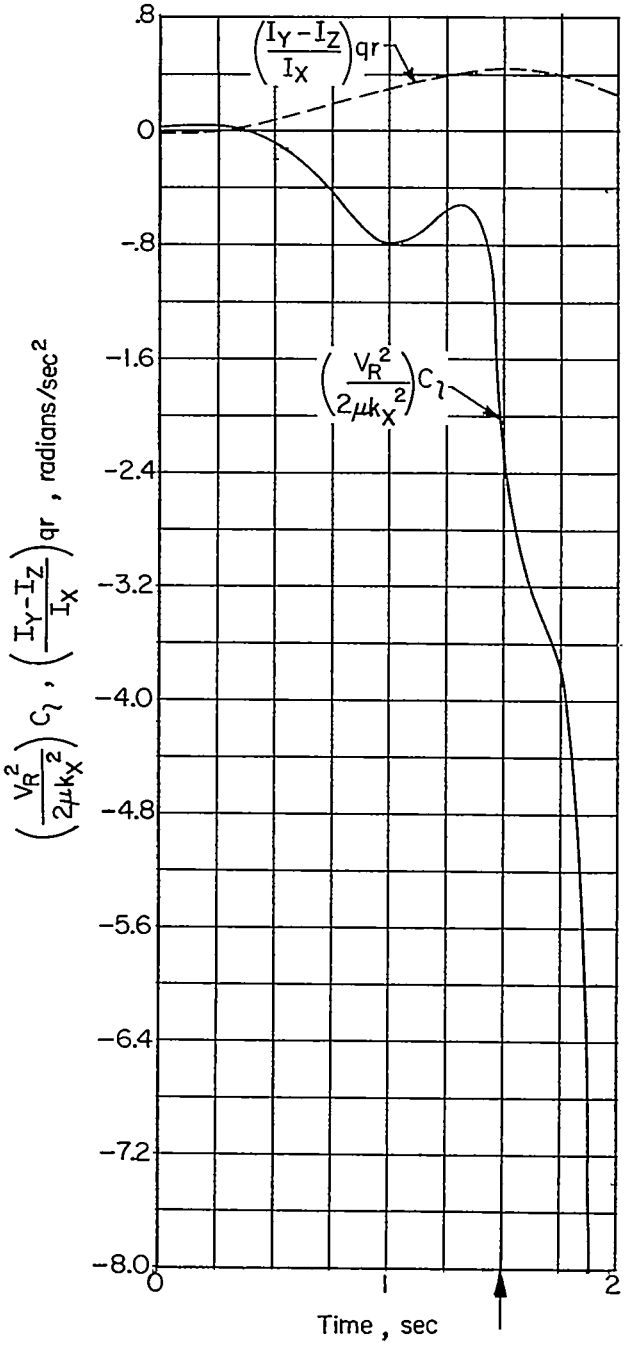

(a) $\dot{p}$ terms where $\dot{p} = \left(\frac{V_R^2}{2\mu k_X^2}\right)C_l + \left(\frac{I_Y - I_Z}{I_X}\right)qr$.

Figure 11.- Calculated time histories of the terms composing the angular accelerations about the X, Y, and Z body axes for the condition where 40,000 foot-pounds of antispin yawing moment was applied. Time at which recovery is completed is indicated by vertical arrow in time scale.

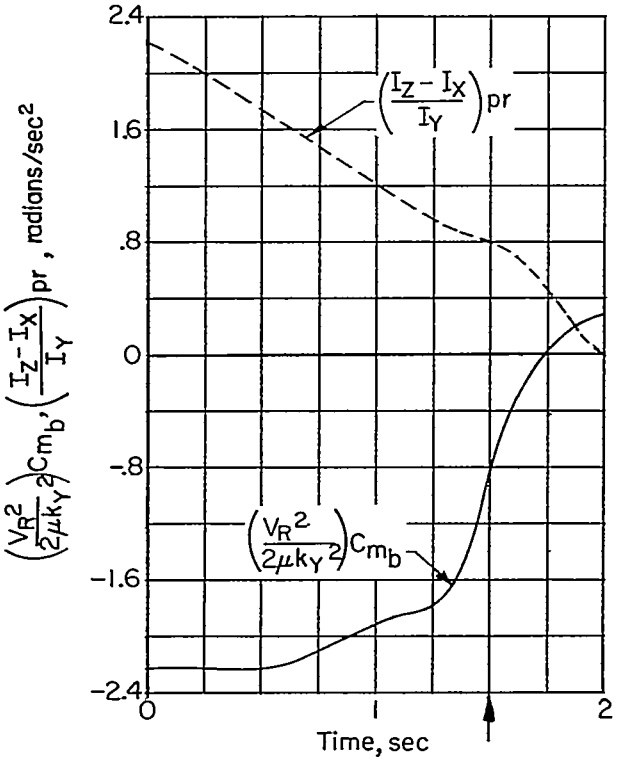

(b) $\dot{q}$ terms where $\dot{q} = \left(\frac{V_R^2}{2\mu k_Y^2}\right)C_{m_b} + \left(\frac{I_Z - I_X}{I_Y}\right)pr$.

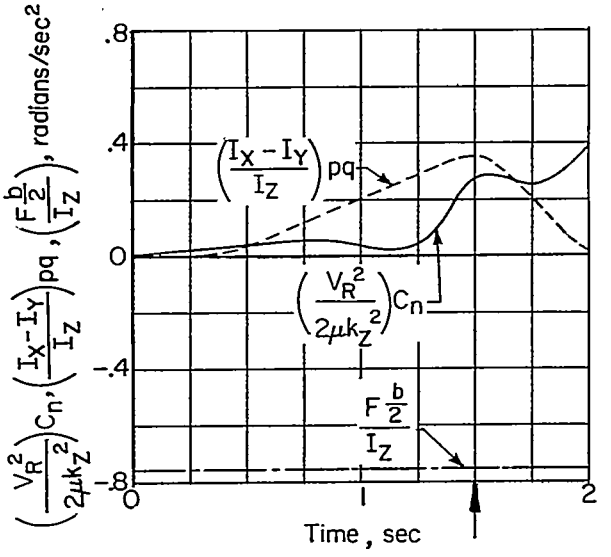

(c) $\dot{r}$ terms where $\dot{r} = \left(\frac{V_R^2}{2\mu k_Z^2}\right)C_n + \left(\frac{I_X - I_Y}{I_Z}\right)pq + \frac{F\frac{b}{2}}{I_Z}$.

Figure 11.- Concluded.

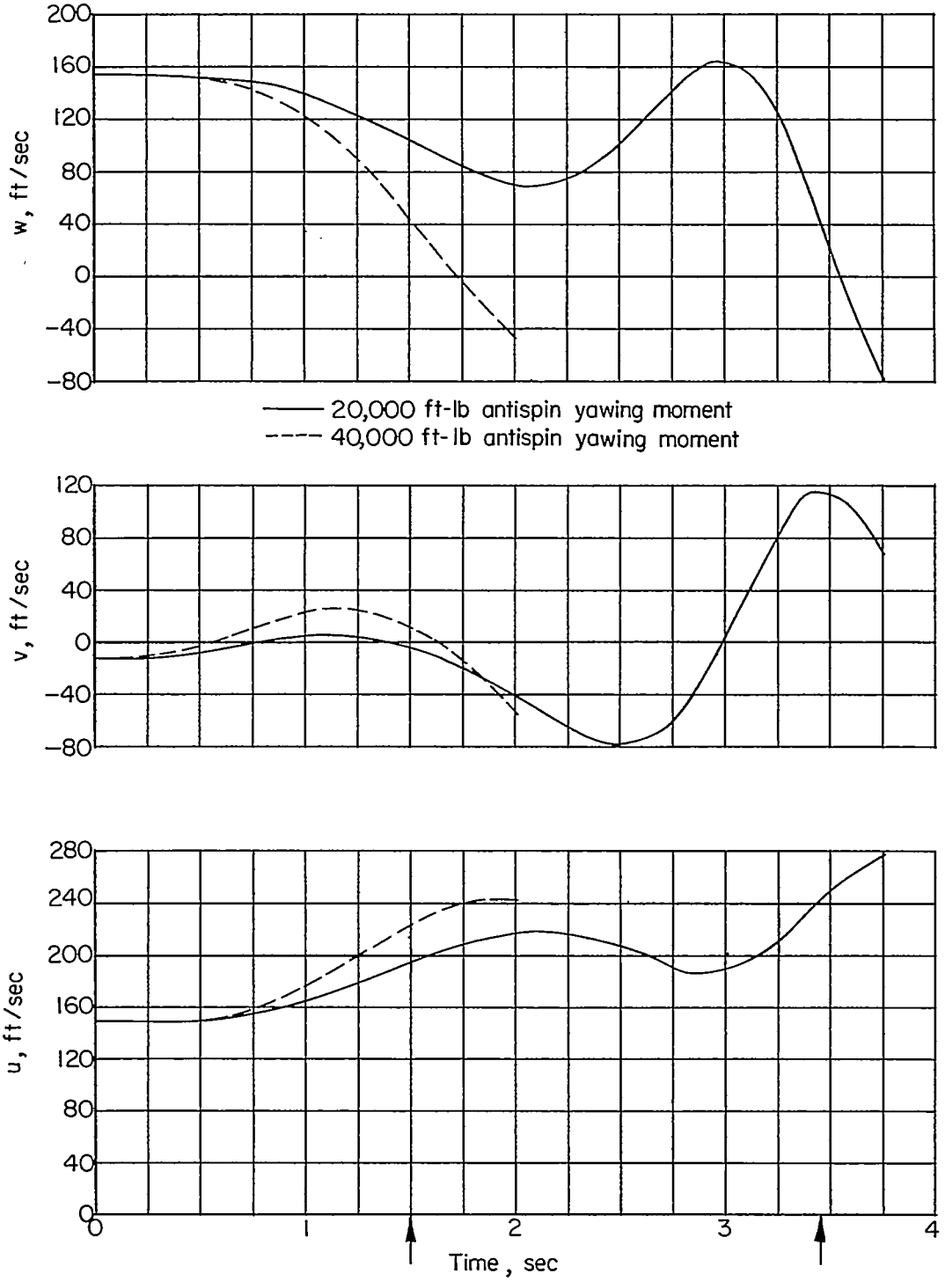

Figure 12.- Calculated time histories of the linear velocities along the X, Y, and Z body axes for two applied antispin yawing moments. Time at which recovery is completed is indicated by vertical arrows in time scale.

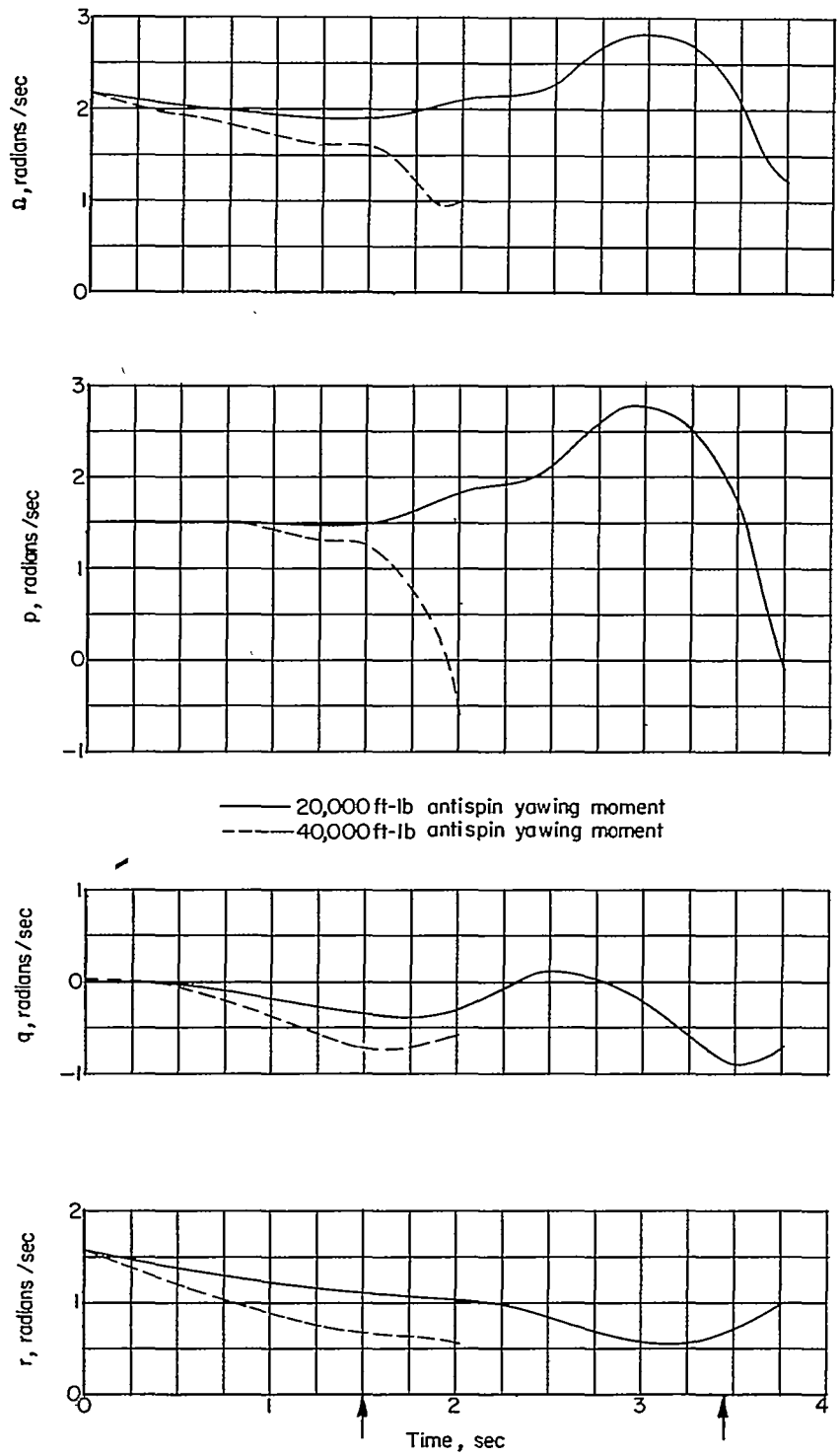

Figure 13.- Calculated time histories of the angular velocities for two applied antispin yawing moments. Time at which recovery is completed is indicated by vertical arrows in time scale.

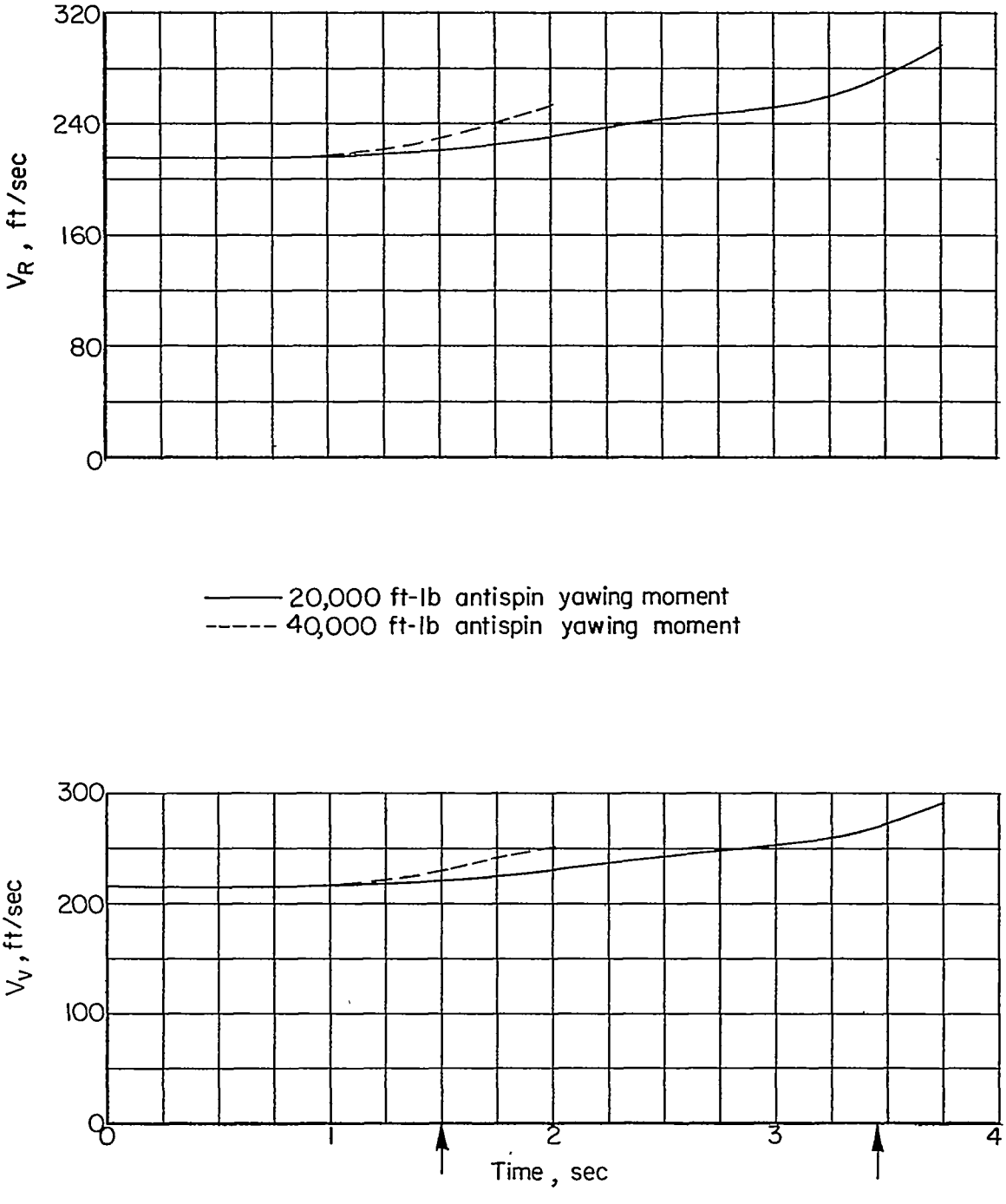

Figure 14.- Calculated time histories of V_R and V_V for two applied antispin yawing moments. Time at which recovery is completed is indicated by vertical arrows in time scale.

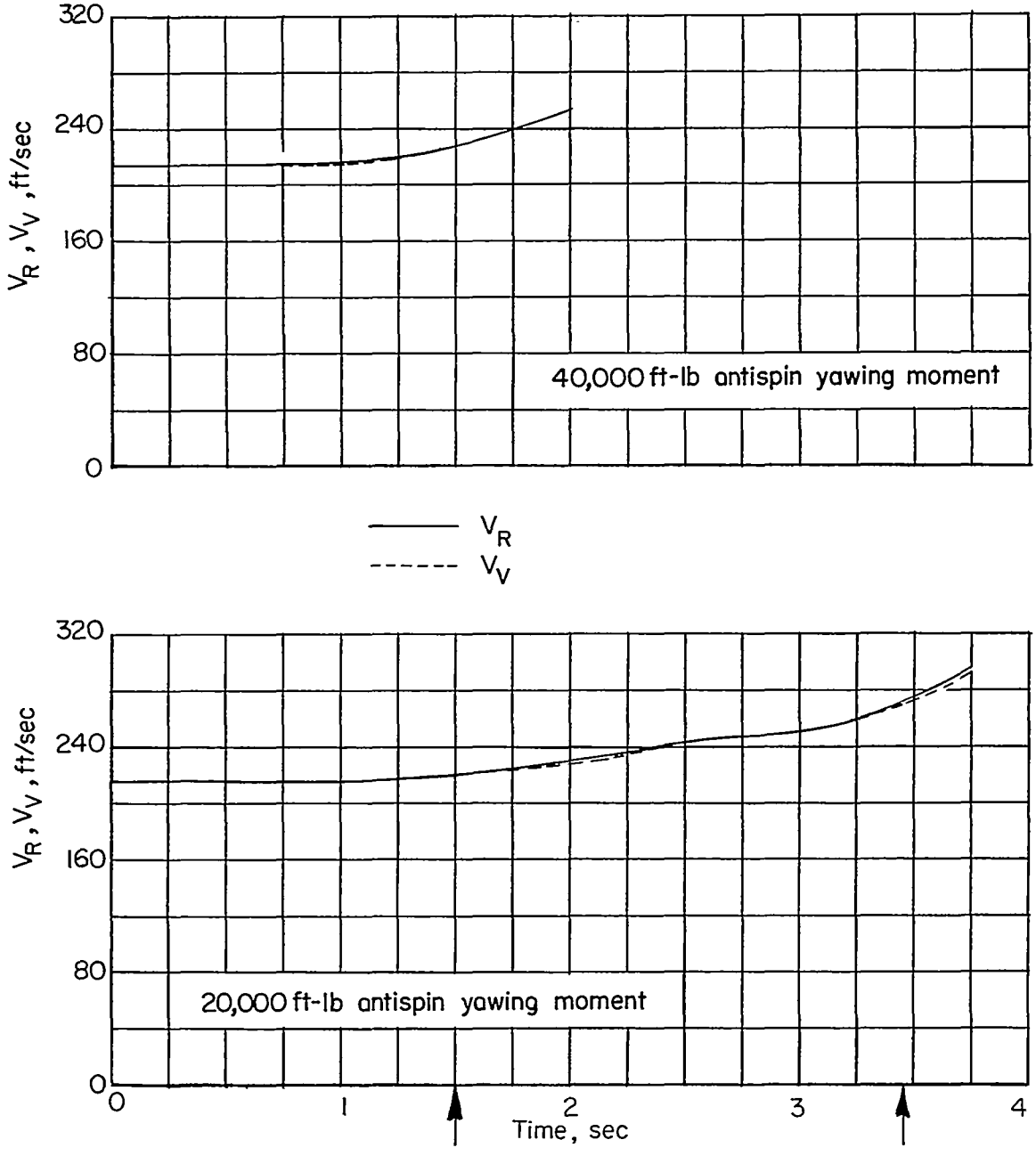

Figure 15.- Comparison of the calculated time histories of V_R and V_V for two applied antispin yawing moments. Time at which recovery is completed is indicated by vertical arrows in time scale.

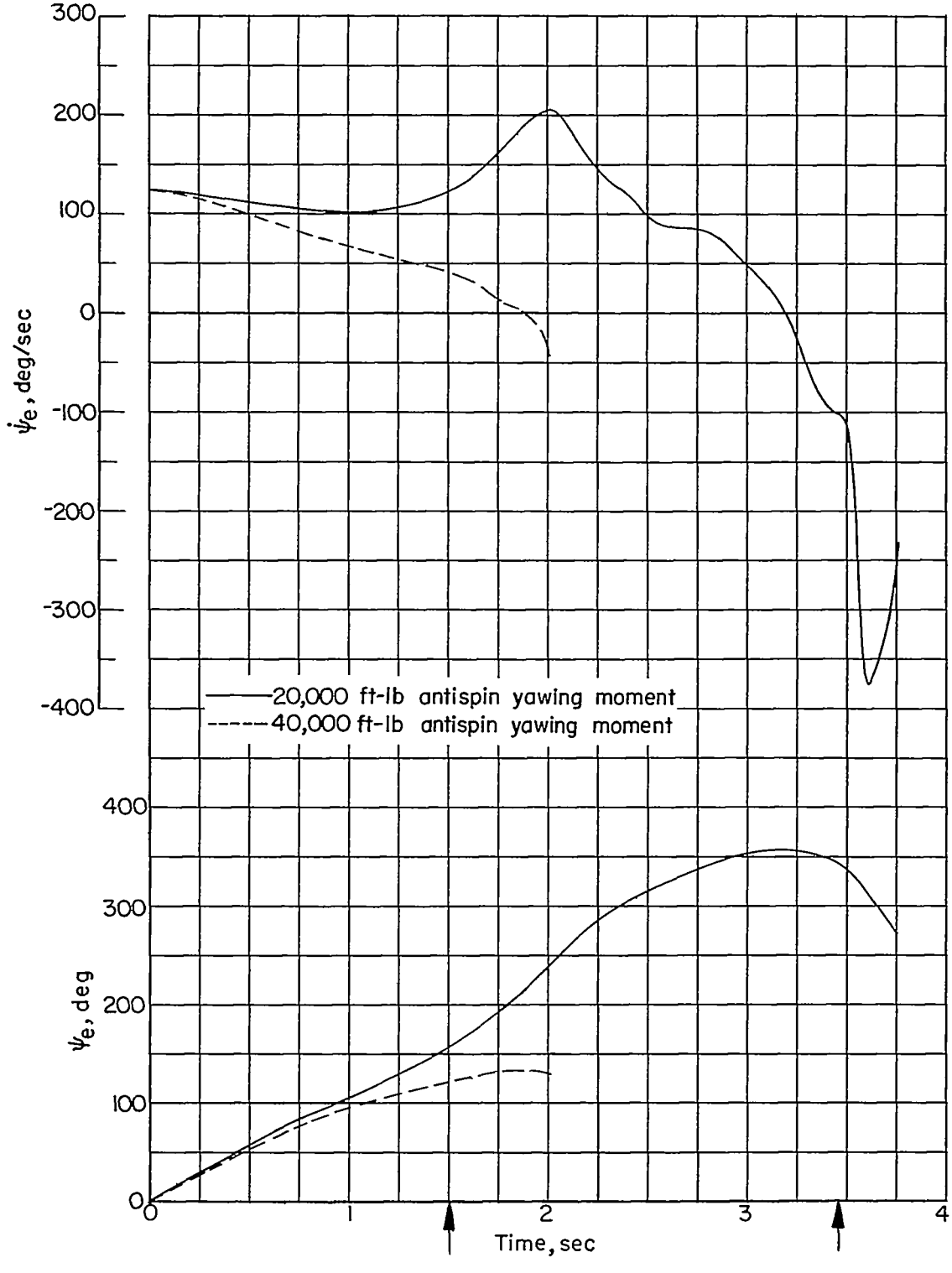

Figure 16.- Calculated time histories of $\dot{\psi}_e$ and ψ_e for two applied antispin yawing moments. Time at which recovery is completed is indicated by vertical arrows in time scale.

NACA-Langley - 12-22-54 - 1000